

Water and carbon stable isotope records from natural archives : a new database and interactive online platform for data browsing, visualizing and downloading.

Timothé Bolliet¹, Patrick Brockmann¹, Valérie Masson-Delmotte¹, Franck Bassinot¹, Valérie Daux¹, Dominique Genty¹, Amaelle Landais¹, Marlène Lavrieux², Elisabeth Michel¹, Pablo Ortega³, Camille Risi⁴, Didier M. Roche¹, Françoise Vimeux^{1,5}, Claire Waelbroeck¹.

1 - Institut Pierre Simon Laplace / Laboratoire des Sciences du Climat et de l'Environnement, LSCE/IPSL, CEA-CNRS-UVSQ, Université Paris-Saclay, F-91191 Gif-sur-Yvette, France.

2 - Eawag, Swiss Federal Institute of Aquatic Science and Technology, Überlandstrasse 133, 8600 Dübendorf, Switzerland.

3 - Laboratoire d'Océanographie et du Climat : Expérimentations et Approches Numériques (LOCEAN) Université Pierre et Marie Curie, 4 Place Jussieu, 75252 Paris, France.

4 - Laboratoire de Météorologie Dynamique (LMD), place Jussieu, 75252 Paris Cedex 05, France.

5- Institut de Recherche pour le Développement (IRD), Laboratoire HydroSciences Montpellier (HSM), UMR 5569 (CNRS-IRD-UM1-UM2), 34095 Montpellier, France.

Correspondence to: T. Bolliet (Timothe.Bolliet@lsce.ipsl.fr)

Abstract

Past climate is an important benchmark to assess the ability of climate models to simulate key processes and feedbacks. Numerous proxy records exist for stable isotopes of water and/or carbon, which are also implemented inside the components of a growing number of Earth system model. Model-data comparisons can help to

constrain the uncertainties associated with transfer functions. This motivates the need of producing a comprehensive compilation of different proxy sources. We have put together a global database of proxy records of oxygen ($\delta^{18}\text{O}$), hydrogen (δD) and carbon ($\delta^{13}\text{C}$) stable isotopes from different archives: ocean and lake sediments, corals, ice cores, speleothems and tree-ring cellulose. Source records were obtained from the georeferenced open access PANGAEA and NOAA libraries, complemented by additional data obtained from a literature survey. About 3,000 source records were screened for chronological information and temporal resolution of proxy records. Altogether, this database consists of hundreds of dated $\delta^{18}\text{O}$, $\delta^{13}\text{C}$ and δD records in a standardized simple text format, complemented with a metadata Excel catalog. A quality control flag was implemented to describe age markers and inform on chronological uncertainty. This compilation effort highlights the need to homogenize and structure the format of datasets and chronological information, and enhance the distribution of published datasets that are currently highly-fragmented and scattered. We also provide an online portal based on the records included in this database with an intuitive and interactive platform (<http://climateproxiesfinder.ipsl.fr/>), allowing one to easily select, visualize and download subsets of the homogeneously-formatted records that conform this database, following a choice of search criteria, and to upload new datasets. In the last part, we illustrate the type of application allowed by our database by comparing several key periods highly investigated by the palaeoclimate community. For coherency with the Paleoclimate Modelling Intercomparison Project (PMIP), we focus on records spanning the past 200 years, the mid-Holocene (MH, 5.5-6.5 ka; calendar kilo years before 1950), and the Last Glacial Maximum (LGM, 19-23 ka), and those spanning the last interglacial period (LIG, 115-130 ka). Basic statistics have been applied to characterize anomalies between these different periods. Most changes from the MH to present day, and LIG to MH appear statistically insignificant. Significant global differences are reported from LGM to MH with regional discrepancies in signals from different archives and complex patterns.

1. Introduction

In the context of increasing anthropogenic greenhouse gas emissions, exploring future climate change risks relies on climate models (IPCC AR5, 2013), and it

61 becomes essential to assess their intrinsic skills and limitations (Braconnot et al.,
62 2012; Flato et al., 2013).

63 Past climate variations resulted from the changing natural external forcings, and
64 internal climate variability. Quantitative records of past climate variations therefore
65 provide unique benchmarks against which it is possible to assess the ability of
66 climate models to resolve the processes at play (e.g. Braconnot et al., 2012, Schmidt
67 et al., 2014). However, evaluating climate models against paleoclimate data remains
68 challenging, due to uncertainties on both simulations and reconstructions (Masson-
69 Delmotte et al., 2013; Flato et al., 2013). On the one hand, uncertainties associated
70 with the simulation of past climates are related to changes in boundary conditions
71 (e.g. ice sheet topography and melt fluxes, <https://pmip3.lscce.ipsl.fr/>) and dust
72 radiative feedbacks (Rohling et al., 2012). On the other hand, uncertainties also arise
73 from the age scales of proxy records, and from the application of transfer functions
74 used to convert proxy records into climate variables. For instance, while $\delta^{18}\text{O}$ is used
75 as a temperature proxy in polar ice cores, the relationship between ice core $\delta^{18}\text{O}$ and
76 temperature is known to vary through time and between drilling sites (Masson-
77 Delmotte et al., 2011a; Guillevic et al., 2013; Buizert et al., 2014). Similarly, the
78 relationship between $\delta^{18}\text{O}$ from tree rings cellulose and climate may be impacted by
79 several factors, including local monthly or annual temperature and precipitation, while
80 the response of trees to climate changes may differ according to inherent
81 physiological differences of the various tree species (Stuiver and Braziunas, 1987;
82 McCarroll and Loader, 2004).

83 In order to constrain the second source of uncertainty, a growing number of
84 components of climate models are being implemented with the explicit simulation of
85 tracers such as water and carbon stable isotopes. Since the pioneer work of
86 Joussaume et al. (1984), many models are being equipped with $\delta^{18}\text{O}$, δD and also
87 $\delta^{17}\text{O}$ water isotopes, including land surface models (Yoshimura et al., 2006;
88 Henderson-Sellers et al., 2006), regional atmospheric models (Sturm et al., 2010)
89 general circulation models (Schmidt et al., 2007 for the coupled ocean-atmosphere
90 GISS model; Lee et al., 2008 for NCAR CAM2; Tindall et al., 2009 for HadCM3; Risi
91 et al., 2010 for LMDZ4; Werner et al., 2011 for ECHAM5wiso; Yoshimura et al., 2011
92 for IsoGSM; Dee et al., 2015) as well as intermediate complexity climate models

(Roche et al., 2013 for iLOVECLIM). Similarly, carbon stable isotopes are also implemented in a growing number of land surface and ocean components (e.g. Tagliabue et al., 2009; Menviel et al., 2012; Sternberg et al., 2009). These new functionalities of climate models open the possibility to directly comparing the proxies measured in natural archives with model output, with the double interest of improving the understanding of proxy records, and model evaluation. For instance, Risi et al. (2010) evaluated LMDZ4 performance against oxygen stable isotope data from terrestrial and ice archives for the MH and LGM, and Oppo et al. (2007) compared the GISS Model-E output with Pacific marine $\delta^{18}\text{O}$ records encompassing the MH. Recently, Caley and Roche (2013) have focused on the difference between the LGM and the Late Holocene (last 1000 years) for the comparison of the simulation from the iLOVECLIM model and proxy data, and selected 17 polar ice core records, 10 speleothems, and 116 deep sea cores with a test on age control following the protocol previously applied for the synthesis of temperature reconstructions by the Multiproxy Approach for the Reconstruction of the Glacial Ocean surface (MARGO) collaborative effort (Waelbroeck et al., 2009). Also, Jasechko et al. (2015) compiled 88 isotope records from ground water, speleothems and ice cores spanning the period from the LGM to the Late Holocene and compared these data to five general circulation models. These model-data comparisons have only used limited information extracted from a fraction of available proxy records, while much broader information has been accumulated during decades of field and laboratory work worldwide.

The main open-access databases are hosted on the NOAA (<http://www.ncdc.noaa.gov/data-access/paleoclimatology-data>) and PANGAEA (<http://www.pangaea.de>) websites. These multi-proxy online data depositories are continuously updated with recent datasets uploaded by the respective authors on a voluntary basis. In some cases, datasets are also available as supplementary information to publications, and practices depend on communities. For instance, there is no standard practice for archiving the growing number of stable isotope records obtained from tree ring cellulose, even though some efforts emerged recently to create a data bank (Csank, 2009). Although the two repositories have been intensively used by scientists to archive and distribute their datasets, the systematic exploration of these records remained limited by the heterogeneity of reporting, data

formats including chronological information, and the impossibility to easily download all the datasets related to one type of proxy. Moreover, these databases have limited interactivity. The lack of features allowing an online pre-visualization of selected datasets obliges the users to download the data if they want to assess the relevance of the records for their scientific questions (e.g. to explore the resolution of the records, or the quality of the chronology for a given time interval). Altogether, unintuitive ergonomics and/or limited interactivity make data browsing and gathering fastidious.

Based on this observation, we decided to produce a compilation of existing records, standardising the chronological information (age markers) into a common format, and implementing an online tool to facilitate the search process throughout different archives with intuitive data browsing, online functions for datasets graphical pre-visualization, as well as easy download features. In a first step, we focus here on $\delta^{18}\text{O}$, δD and, if available on the same archive, $\delta^{17}\text{O}$ and $\delta^{13}\text{C}$. This choice is motivated by the following reasons: (i) these proxies have been widely used during the last decades; (ii) they are available for a variety of marine, ice and terrestrial archives (sediments, speleothems, ice and tree-ring cellulose), and (iii) they trace interactions between different components of the climate system involved in the global water and carbon cycles, and provide therefore integrated signals for evaluating respectively water and carbon cycle processes within climate simulations. A strong motivation for this compilation is the integration of marine and terrestrial records (Bar-Matthews et al., 2003; Hughen et al., 2006; Cruz et al., 2006; Leduc et al., 2009; Carré et al., 2012; Bard et al., 2013; Grant et al., 2012 & 2014). It is also in line with ongoing efforts to build consistent chronologies for marine and ice core records (e.g. the INTIMATE project, see Blockley et al., 2012). In order to document the four dimensional structure of ocean circulation changes, we included datasets from deep-sea sediments, using both surface and deep water proxies.

While in principle our methodology could allow one to explore transient climatic changes (Marcott et al., 2013; Shakun et al., 2012), such an approach would require an accurate assessment of age scale uncertainties, which is beyond the scope of this work. In this manuscript, we therefore focus on records providing sufficient age control and resolution for selected time slices, chosen for consistency with the Paleoclimate Modelling Intercomparison Project (PMIP), and for which numerous

source records are available. The selection of target periods is described in Section 2. The protocols and methods used to build the database are then depicted in Section 3, followed by the description of the software developments required for the online search and visualization platform (Section 4). For the four considered time slices, we then illustrate the data coverage and spatial distributions (Section 5). Conclusions provide recommendations to facilitate such data syntheses, and propose future database developments.

2. Selection of target periods

Although the database contains full length published records, allowing the investigation of transient climatic changes, our data synthesis in the frame of this manuscript is focused on key periods for which there is a specific interest in the paleoclimate modeling community: the last 200 years, the Mid-Holocene (MH; 6 ka), the Last Glacial Maximum (LGM) and the last interglacial period (hereafter LIG). The methodology used to estimate the isotopic offset between the different periods and the determination of its significance are provided in the appendix.

The last 214 years (1800 to 2013 CE, Common Era, noted as “last 200 years” for simplification) have been selected because (i) they encompass instrumental measurements (precipitation or seawater isotopic composition, air and water temperature, rainfall, sea level pressure...), and because (ii) isotopic atmospheric models can be nudged towards atmospheric historical reanalyses, thus providing a realistic framework for model-data comparisons (e.g. Yoshimura et al., 2008). It is here in fact extended back to 1800 to encompass, if possible, the climate response to the large 1809 and 1815 volcanic eruptions. This period is particularly important for detection and attribution of climate change, and, so far, the short duration of isotopic measurements in precipitation samples (i.e. at best 60 years for $\delta^{18}\text{O}$ in central Europe; Araguas-Araguas et al., 2000; GNIP Database, IAEA/WMO, 2015), has limited systematic investigation of recent trends. Here, we aim at expanding this documentation from highly-resolved proxy archives (mostly ice cores and tree-ring cellulose). Note that the records do not necessarily span the entire key periods (i.e. a record spanning only the last 50 years would be included in our statistics for the present-day period).

The MH (6 ± 0.5 ka, thousand years before 1950) has been selected as a target for paleoclimate modeling (<https://pmip3.lsce.ipsl.fr>) as a compromise between the magnitude of orbital forcing, and climate responses at the end of the glacial ice sheet decay. The orbital configuration produces enhanced (reduced) insolation in the northern (southern) hemisphere during boreal (austral) summer, associated with warming in mid and high northern hemisphere latitudes as well as enhanced northern hemisphere monsoons (Braconnot et al., 2012). So far, most quantitative model-data comparisons for this period have focused on sea surface (Hessler et al., 2014) or surface air temperature inferred from marine and pollen data, and precipitation changes inferred from pollen or lake level data (Harrison et al., 2013). They suggest that models tend to underestimate the magnitude of latitudinal temperature gradients, as well as the magnitude of continental precipitation changes (Flato et al., 2013). While the signal-to-noise ratio is often small, this recent period is well documented in many well-dated, high-resolution archives, motivating a synthesis of proxy information.

The LGM (19-23 ka) corresponds to a major global climate change, in response to decreased greenhouse gas concentration and expanded continental ice sheets, with an amplitude of global cooling of around 4°C , comparable to the magnitude of projected 21st century high-end warming (Collins et al., 2013). Due to the magnitude of the radiative perturbation associated with changes in atmospheric composition and ice sheet albedo, this period is particularly relevant for climate sensitivity (Masson-Delmotte et al., 2013; Rohling et al., 2012; Schmidt et al., 2014). Moreover, the LGM has been widely investigated through well-preserved natural archives with improved chronologies (Reimer et al., 2013). A synthesis of marine data has been achieved within the MARGO collaborative effort (Waelbroeck et al., 2009), leading to a database of multi-proxy sea surface temperature estimates, complementing surface air temperature change between the LGM and present-day inferred from pollen and ice core records (Braconnot et al., 2012). This period is marked by changes in the thermohaline circulation (Duplessy et al., 1988; Shin et al., 2003; Yu et al., 1996), large scale atmospheric circulation (Chylek et al., 2001; Justino and Peltier, 2005; Murakami et al., 2008), El Niño - Southern Oscillation (ENSO; Tudhope et al., 2001; Stott et al., 2002) as well as the monsoon and Inter-Tropical Convergence Zone (ITCZ) position (Van Campo, 1986; Braconnot et al., 2000; Broccoli et al., 2006;

Leduc et al., 2009; Bolliet et al., 2011; Sylvestre, 2009). The large uncertainties associated with changes in ocean circulation and their role for the carbon cycle and the tropical water cycle have already motivated data syntheses and model-data comparisons (Bouttes et al., 2012; Caley et al., 2014, Risi et al., 2010).

Finally, the last interglacial period (115-130 ka) is characterized by large changes in orbital forcing, together with reduced volume of the polar ice sheets (Kukla et al., 2002; Govin et al., 2012; Masson-Delmotte et al., 2013; Capron et al., 2014). While global mean temperature is estimated to be less than 2°C warmer than today, based on syntheses of temperature reconstructions and simulations (Otto-Bliesner et al., 2013), northern hemisphere summer warming in this period can reach the same magnitude of feedbacks than in future projections (Masson-Delmotte et al., 2011a). It is also characterized by enhanced inter-hemispheric and seasonal contrasts (Nikolova et al., 2013). Large uncertainties also reside on the conversion of Greenland and Antarctic ice core water stable isotope records to temperature, with implications for assessing the vulnerability of ice sheets to local warming (Masson-Delmotte et al., 2011a; Sime et al., 2009 & 2013; NEEM community members, 2013). Climate models have been shown to underestimate the magnitude of Arctic warming and to fail capturing Antarctic temperature trends (Lunt et al., 2013; Bakker et al., 2014). This may arise from vegetation and land ice feedbacks, which were not resolved in the simulations. While all of the above motivate a proxy record synthesis for this period, highly-resolved archives remain scarce (Pol et al., 2014), and large age-scale uncertainties constitute a major obstacle, especially given the asynchronous climate change detected in both hemispheres (Stocker, 1998; Masson-Delmotte et al., 2010; Bazin et al., 2013; Capron et al., 2014).

3. Database construction steps

The first step consisted in gathering all the $\delta^{18}\text{O}$, $\delta^{13}\text{C}$ and δD data available from the two main online paleoclimate data depositories (NOAA and PANGAEA), together with marine sediment records from the LSCE (Gif-sur-Yvette, France), paleoceanography internal database (Caley et al., 2014) and literature survey and

personal communication (2013,2014) with authors. This work was performed from May 2013 to July 2014.

A metafile has been built in order to list the main parameters of these datasets: core name, reference, associated publication Digital Object Identifier (DOI), core site latitude, longitude and elevation or depth coordinates. We have also inserted a flag to describe the quality of age models for marine sediment cores (see next section). All ages were converted into thousand years before present (ka), using 1950 CE as the reference year. For each archive, we have stored the depth / age / proxy value data into a separate three-column file. This protocol was applied to each archive and proxy record. For instance, for a publication reporting $\delta^{18}\text{O}$ time series based on four different foraminiferal species, extracted from two deep sediment cores, we have produced eight files, using a simple text tabulated standard format. This standardization was adopted in order to facilitate the comparison of records, and to allow future automated calculations. The name of this standard data file was inserted into the metafile. The name of output files was established based on the name of the original file provided by authors. We thus simply added the acronym "SIMPL" (for "simplified") to the data-only file name. For publications presenting several records, the different cores, species and/or proxies were indicated to the individual data files. For instance, "*stott2007_MD81_cmund_corrected_SIMPL*" and "*Stott2007_MD81_cmund_SIMPL*" are the output files for the $\delta^{18}\text{O}$ records from core MD98-2181 published by Stott et al. (2007), based on the benthic foraminifera *Cibicidoides mundulus* with and without adjustment for vital effect, respectively.

All the available information describing the associated age model was extracted and compiled into a separate spreadsheet named after the original data file, with the addition of the "TIEPTS" (for "tie points") to the file name, as well as the core reference in case of articles based on multiple records. This spreadsheet contains sample reference and depth, raw and/or calendar ages from radiometric dating with the name of the species or the type of material measured, tie points used for core-to-core correlation, and the amount of dated material. The name of this file was also listed in the metafile, and this information was used to evaluate the age model (see next section).

This database was used to calculate basic statistics (number of data points, average proxy value, standard deviation) for the MH, the LGM, the last Interglacial, and for the reference present-day climate (last 200 years).

4. Age model evaluation

4.1 Deep sea sediment cores

Following the protocol developed for the MARGO project (Waelbroeck et al., 2009), quality flags were attributed to the chronology of the deep sea sediment cores and speleothems. For this purpose, several factors were taken into account:

1. The density of chronologic markers: AMS ^{14}C and/or U-Th dates, core-to-core correlation tie points, reference horizons (tephra, paleomagnetic excursions...).

2. The position of age markers, especially at the boundary of our target periods. For instance, we consider that the LGM (19-23 ka) is better constrained with two AMS ^{14}C dates at 19 and 23 ka than with four dates within the 20-22 ka interval.

3. The presence of sedimentary disturbances (turbidites, hiatus, bioturbation) and post-deposition or coring events (gaps, core breaks, post-deposition reorganization of speleothems crystals). This aspect of the age-model evaluation is however restricted to the information provided by authors concerning the possible presence of such disturbances.

4. The level of detailed description of the age model: raw ^{14}C and U-Th ages, samples reference, type of material or species analyzed, reservoir age and calibration program or curve used in case of marine material. Reservoir ages still remain vigorously discussed (Soulet et al., 2011; Siani et al., 2013). Here, we used the reservoir ages as originally published.

5. Marine Core-top constraints. It is customary among paleoceanographers to assign "0 BP" to the uppermost sample of the core. Many late Holocene records are also

dated using extrapolated ages between the most recent datum and the top of the core. This implies that the top of deep-sea cores is often poorly chronologically constrained. Although arbitrarily dated, these data points were integrated to the calculation of present-day average values.

6. For records older than the ^{14}C reliability interval (~35 ka to 60 ka, where the uncertainty on the calibration into calendar ages strongly increases, Plastino et al., 2001; Bronk-Ramsey et al., 2013), the quality flags are based on the number of tie points, and the type of material used for core-to-core correlation (e.g.: well dated high resolution ice core vs. low resolution sediment core).

Quality flags ranging from 1 (very good) to 5 (poor) were therefore included in the metafile for each deep-sea sediment core and speleothem dataset. This evaluation protocol was not applied to archives such as tree rings, varved lacustrine cores, high accumulation ice cores, modern corals or mollusk shells where annual counting allows building accurate chronologies. We thus assigned the best quality flag to these records.

In order to illustrate the chronological quality flag, we describe hereafter five examples:

a) Quality flag 1 (excellent): Marine Core A7 (27.82°N, 126.98°E investigated by Sun et al., 2005) is constrained by 15 well-distributed AMS ^{14}C dates ranging from 1 to 17.5 ka, corresponding to the time period where oxygen stable isotope data are available. There is therefore no significant arbitrary-dated interval. The authors used a dated ash layer to establish a precise correction of the theoretical reservoir age, and the effect of local turbidites was precisely monitored. The dating protocol is described in detail, and reports samples labels, reservoir age, and the calibration curve. Despite the lack of information on the selected species and the amount of material used for ^{14}C dating, we assigned the maximum quality flag to this age model.

b) Quality Flag 2 (good): Marine Core GEOB3129/3911 (4.61°S, 36.64°W) is dated through 16 AMS ^{14}C dates spanning the 1.8-20 ka interval, which coincides with the

period covered by isotope measurements (Weldeab et al., 2006). The dating protocol is relatively well described although reservoir ages and the amount of measured material are not directly mentioned. With one date at 20 ka and another one at 16.9 ka, the distribution of dates does not provide a precise picture of the timing of the starting date of the last deglaciation.

c) Quality Flag 3 (average): Marine Core KNR159-5-33GGC (27.56°S, 46.18°W; Tessin and Lund, 2013) is constrained by 14 AMS ^{14}C dates between 1.6 and 18.5 ka, and the entire dating protocol is well described. However, the AMS ^{14}C dates are not homogeneously distributed, with only 4 data points within the 1.6-14 ka interval and 10 dates between 15.4 and 18.5 ka. The chronology of the Holocene is therefore poorly constrained. Moreover, anomalously old material is intercalated between younger sediment, interpreted as deep burrying (Sortor and Lund, 2011).

d) Quality Flag 4 (below average): the age scale of Core RC10-196 (54.70°N, 177.08°E) is particularly well described by Kohfeld and Chase (2011). However, only three AMS ^{14}C dates and one $\delta^{18}\text{O}$ data point for oxygen isotope stratigraphy are available between 10 and 22 ka, while the $\delta^{13}\text{C}$ and $\delta^{18}\text{O}$ records span a considerably wider time interval (10-86 ka). The starting point of Termination I is not well defined in $\delta^{18}\text{O}$, making the datum at 22 ka relatively imprecise. Although the authors did not focus on the last deglaciation, we incorporated this record in the database, because only very few records have been recovered in this part of the North Pacific.

e) Quality Flag (poor): $\delta^{18}\text{O}$ record from Core M44/3_KL83 (32.60°N, 34.13°E; Sperling et al., 2003) spanning the last 13 kyrs. This record is constrained by only one ^{14}C AMS date (7.6 ka), leading to large uncertainties in the timing of the whole Holocene.

4.2 Other archives

Ice cores

Dating ice cores is a crucial issue, as these highly-resolved archives are often compared to marine cores and speleothems to assess the timing of climatic events

between high and lower latitudes. Ice core chronologies are regularly updated using available age markers and dating is synchronized among different ice cores (e.g. Rasmussen et al., 2006; Vinther et al., 2006; Ruth et al., 2007; Bazin et al., 2013; Veres et al., 2013), with estimates of associated age scale uncertainties. For that reason, it was decided not to attribute dating quality flags for ice cores chronologies in this database. For the last interglacial period, LGM and MH, most ice cores chronologies would be flagged as good to excellent, depending on the dating strategy. For the last 200 years, the quality of ice core chronologies can vary from excellent for high accumulation areas (where annual layer counting and volcanic horizons are available) to good in the driest central Antarctic areas.

Speleothems

Dating speleothems generally involves radiometric methods or, in rare cases, counting of annual laminae when they are visible. In the majority of cases, it is based on uranium series methods (schematically ^{234}U decays into thorium ^{230}Th); when the U/Th method is not possible because of too large detrital content, some authors may use AMS ^{14}C with a correction of dead carbon producing quite large errors. U-Th method on speleothems can have a <1% 2-sigma error bar and the age limit of the method is close to 450 ka; but depending on the detrital content of the calcite and on the method used (i.e. TIMS, MC-ICPMS or alpha counting for old records), errors may be variable. Chronologies based on radiometric dating were evaluated similarly to what was done with marine cores, with quality flags based on the resolution and distribution of the dated samples, and taking into account the possible sedimentary issues (recrystallizations, hiatus not caused by climate fluctuations). In the case of dating by lamina counting, similarly to what was done to modern coral records, we considered that the error on the chronology is low, and assigned the maximum quality flag to the age model of these cores.

Lacustrine records

The construction of age models for lacustrine cores is somewhat similar to what is applied for marine cores. Most of the chronologies are based on AMS ^{14}C dating measured on carbonate or organic compounds. Similarly to what was performed for marine datasets, the quality flags for lacustrine records are based on the density of

¹⁴C dates and their position relatively to key transitions. We also took the sedimentary disturbances (e.g. sedimentation hiatuses) into account as well as the presence of potential corrections for residence time and reservoir effects revealing an effort for considering the impact of the lake circulation dynamics in the sediment age. The chronology of some of the compiled lacustrine records was performed by counting of seasonal varve, generally resulting in a high accuracy (Sprowl, 1993). As a result, we attributed the “excellent” quality flag to varve-based chronologies.

Tree-ring records

Tree-ring are generally short and well-dated records. The dating method is based on precise counting of single rings produced each year by individual trees. Although some chronologies can be affected by a few double or missing rings, tree-rings may be the archive presenting the most robust chronologies and allow the attribution of a precise calendar year to each of the rings. We therefore assigned the “excellent” quality flag to all of the tree-ring records of our database.

5. Interactive visualization tool

NOAA and PANGEA open-access online libraries host a huge amount of palaeoclimatic datasets, but browsing and downloading these data may sometimes not be optimal. Each dataset must indeed be downloaded individually, without having the possibility to quickly visualize the records online.

This is particularly critical when users need to download a large amount of records not corresponding to a specific site and/or author. This lead us to develop a tool that optimizes the datasets browsing step, with an online data plotting function, and a user-friendly tool for downloading multiple datasets.

One of the main objectives of this application (<http://climateproxiesfinder.ipsl.fr/>) is to ease exploration of multi-dimensional data assembled from mutiple proxy records containing common features. This approach is relatively new and benefits from the latest interactive data visualization techniques (d3.js [<https://d3js.org/>], dc.js

[<https://dc-js.github.io/dc.js/>], Leaflet [<http://leafletjs.com/>], bokeh [<http://bokeh.pydata.org/>]). Fig. 1a shows the layout of the Climate Proxies Finder which consists of a world map (top row) and four charts representing, respectively, the proxy depth, age (oldest, most recent), archive type (ice, lake, ocean, speleothem, tree) and material (e.g. carbonate, coral, etc.). A table of the available records is also displayed at the bottom of the screen (first 100 only). This table displays information about the records (depth, age [most recent, oldest], archive, material, DOI, and the reference of the corresponding scientific paper). The DOI is hyper-linked to the google scholar search engine. The user can interactively filter the dataset by clicking or brushing on any of these charts or by dragging and zooming in and out of the map. Since all charts are inter-connected, they will automatically be updated according to the filter selections. Fig 1b shows an example of this interactive filtering with the selection of ocean archive type near the surface (0 - 500 m). Accordingly, due to the crossfiltering functionality, all other charts and the table reflect only the proxies selected by these filters. This application also allows the user to display an interactive plot of the time series of the available isotopes by clicking on a map marker (see Fig. 1c for an illustration).

Lastly, the user is able to download in a zip file the selected proxy data as CSV files and time series plots by clicking on the shopping cart icon.

The Climate Proxies Finder application continues to evolve as new features are needed, such as adding a filter for proxy chronological information quality.

6. Results

The overall increase in the number of records and publications per year over the last 50 years (Fig. 2) reflects the growing investment in obtaining stable isotopes records to document and understand past climates. The peak in the number of records published in 1998 and 1994 are mostly due to the presence of some publications compiling a large number of previously unpublished marine records from the Atlantic Ocean (Sarnthein et al., 1998; Sarnthein et al., 1994).

6.1 Geographical distribution of data and temporal resolution

This section briefly describes the status of the database for marine and terrestrial records (Fig. 3), and provides a synthesis of stable isotope data for each focus period.

A total of ~6,400 records were collected from the NOAA and PANGAEA data repositories as well as from the internal LSCE database. About 3300 marine records were rejected, as they are not yet published. Following the settings of our online portal, we also isolated about 300 $\delta^{18}\text{O}$ and $\delta^{13}\text{C}$ published records not dated (~200 records) or containing no information about the core site elevation or depth (~100 records). We thus accumulated about 1,700 $\delta^{18}\text{O}$ records from ~900 sites, about 900 $\delta^{13}\text{C}$ records from 450 sites, and about 230 δD records from 60 core sites (with 20 additional deuterium excess records). When considering the different types of archives, we compiled about 1,200 $\delta^{18}\text{O}$ and ~700 $\delta^{13}\text{C}$ records from 600 marine sediment cores, 200 $\delta^{18}\text{O}$ and 75 $\delta^{13}\text{C}$ speleothems records from 60 caves, 200 dated $\delta^{18}\text{O}$ records from 50 ice cores (with about 60 additional dated δD datasets and ~20 $\delta^{17}\text{O}$ records), 60 $\delta^{18}\text{O}$ and 60 $\delta^{13}\text{C}$ lacustrine records (with δD datasets), as well as 85 $\delta^{18}\text{O}$ and 80 $\delta^{13}\text{C}$ records from tree rings.

Among all the 1,900 collected marine records, about 850 do not present any information about the construction of their age model and about 950 records are associated with age model tie points or by default associated with an *excellent* chronology (e.g. modern corals), while most of the lacustrine cores and speleothems are associated to chronological information. We also note that, when not considering tree-rings records, about 500 dated records do not present any sampling depth or distance scale. The absence of the age scale and/or chronological tie-points clearly prevents any comparison with other records or with climate model output. Similarly, the absence of a depth scale prevents the detection of potential sedimentary or chronological issues, and therefore the correction with existing age models.

6.1.1 Geographical distribution

508

509 For each period of interest, although the amount of compiled records is large enough,
510 the geographic distribution of marine cores is not homogenous, as 75% of the $\delta^{18}\text{O}$
511 and $\delta^{13}\text{C}$ dated records are located in the Northern Hemisphere, with a maximum
512 density in the northern sub-tropical band (Fig. 3 and 4). The Atlantic Ocean is the
513 best documented (about half of all marine records). Most of the compiled records for
514 the Indian, Pacific and Southern Oceans come from sediment cores recovered on
515 continental margins, because a part of the seafloor in the open ocean is deeper than
516 the carbonate compensation depth in these basins (Berger and Winterer, 1974), and
517 the sedimentation rate is particularly low in the large oligotrophic areas of the open
518 ocean. This lack of suitable core sites constitutes a critical limitation for the
519 documentation of the past open-ocean circulation and mechanisms affecting the
520 entire Indian and Pacific basins, such as ENSO, latitudinal migrations of the ITCZ,
521 fluctuations in the thermohaline circulation, with possible formation of past North
522 Pacific intermediate and deep water (Mix et al., 1999; Ahagon et al., 2003; Max et al.,
523 2014), and storage of carbon in the Southern Ocean (Skinner et al., 2010; Burke and
524 Robinson, 2011). Vast areas remain virtually undocumented in the Indian, Pacific and
525 Southern Oceans. A large majority (about 90%) of the records of the ocean database
526 are based on foraminifera, while corals are much scarcer and only few studies use
527 molluscs or diatoms.

528

529 The distribution of continental records (Fig. 3) naturally depends on the position of
530 caves, lakes, forests as well as ice sheets and glaciers. Speleothem $\delta^{18}\text{O}$ records are
531 found on each continent, but with a very heterogeneous distribution. In fact, due to
532 the distribution of caves presenting exploitable speleothems, several large areas
533 (Russia and central Asia, northern and tropical Africa, Canada, central South
534 America) remain undocumented, while the density of records is large in Europe,
535 USA, Central America and China. While they have provided highly resolved records
536 of regional climate variability (e.g. the monsoon and ITCZ, circum-mediterranean
537 continental climate), speleothems do not provide a global coverage. Lacustrine
538 records are also very unevenly distributed, with very few dated isotopic records in
539 South America, Africa, Russia and Australia, although these regions present
540 numerous lakes.

Oxygen and carbon stable isotopes from tree rings cellulose have recently emerged as powerful paleoclimate proxies, albeit with heavy sample preparation (Libby et al., 1976; Long, 1982; Ehleringer and Vogel, 1993; Switsur and Waterhouse, 1998). This feature, and the fact that few tree ring isotopes datasets are available online, lead to relatively scarce archives at a global scale. Most of the available records are located in Europe, while the remaining other datasets (mainly $\delta^{13}\text{C}$ records) are restrained to a few sites in Asia, South America, Siberia, Costa Rica and USA. This distribution of records implies that associated large-scale climate reconstructions are somewhat constrained to Europe.

With respect to ice cores, 75% of the compiled $\delta^{18}\text{O}$ and δD are from Greenland and Antarctica. Few cores indeed were recovered from high elevation ice caps and glaciers from the Andes, Alaska, Arctic Russia, Svalbard, Mount Kilimanjaro and the high-latitude Canadian islands, close to Greenland (Fig. 3). We stress the fact that most published ice core records from Tibet spanning the past centuries are not available from open-access sources.

Contrary to the geographical distribution, the vertical distribution of marine cores along the water column is relatively homogenous for the global ocean (Fig. 5), with more than 100 datasets in each of the 500 m-thick layers from the surface down to 4000m, while data are scarce below this level.

6.1.2 Temporal distribution

We now describe the distribution of records throughout the different periods of interest (Fig. 6). Marine $\delta^{18}\text{O}$ and $\delta^{13}\text{C}$ records are well represented over the four periods, with at least 200 records available for each of the time slices. However, many marine sediment core tops are poorly dated, and thus the number of marine data delivering a robust characterization of recent oxygen and carbon isotopic composition is limited. About half of the marine records have only one data point over

the last 200 years (about 50% of the $\delta^{18}\text{O}$ records and 60% of the $\delta^{13}\text{C}$ records) and most of them have fewer than ten data points over the last 200 years (~65% of $\delta^{18}\text{O}$ and $\delta^{13}\text{C}$ records). When considering the other PMIP key periods, it appears that the distribution is similar for the MH (about 90% of the $\delta^{18}\text{O}$ and $\delta^{13}\text{C}$ records have fewer than ten data points), while the resolution is slightly better for the LGM (65% of $\delta^{18}\text{O}$ and 70% of $\delta^{13}\text{C}$ records have fewer than ten data points) and for the large time interval assimilated here to the last interglacial (~50% records have fewer than ten data points).

Speleothem records span a large variety of time-intervals, ranging from seasonal to glacial/interglacial scale. Due to the heterogeneity of the time slices spanned by speleothems records, the information provided is relatively fragmented. As a result, although we compiled more than 200 speleothem $\delta^{18}\text{O}$ records, none of the four key time-slices selected by the PMIP project contains more than 60 records (30 for $\delta^{13}\text{C}$), due to the fact that many records span time intervals are in between these time-slices. Also, only three dated speleothem $\delta^{18}\text{O}$ records span the entire time interval from the last interglacial period to present-day, and only 14 records span both the LGM and the MH. In general, speleothem records have a better temporal resolution than marine records. For each of the four key periods, at least 60% of the records display more than ten data points. One difficulty arises from the fact that exceptionally long speleothem records such as the one obtained from the Hulu and Dongge caves records (Wang et al., 2001; Wang et al., 2005) have been obtained from the compilation of measurements performed on several speleothems/cores from one single cave. These multiple individual cores may present significant and varying offsets which can be identified over different periods of overlap (see Wang et al., 2001 and Yuan et al., 2004). As a result, establishing a robust composite record allowing calculation of anomalies between different past periods is particularly delicate for these archives. For this reason, we decided to keep the individual short datasets separated as they were published, and did not build long and continuous composite records. Therefore, composite records cannot be displayed in our LIG-MH comparison map (Figure 9).

$\delta^{18}\text{O}$ records from ice cores are relatively scarce for the oldest PMIP time slices, with only ~45 records spanning the MH, ~40 for the LGM, and 14 concerning the LIG (13,

13 and 6 for δD , respectively). Only five $\delta^{18}\text{O}$ records are continuous from the LIG to the Holocene. Ice core records however provide a wealth of information on the spatial and temporal variability of surface snow isotopic composition over the last decades, as about 140 of the ~180 compiled $\delta^{18}\text{O}$ dated records spanning the last 200 years exhibit at least ten data points within this period (50 out of 55 dated records for δD and deuterium excess).

As the effect of burial on $\delta^{18}\text{O}$ of fossil wood cellulose remains poorly known (Richter et al., 2008), we selected records exclusively based on living trees or timber wood. Consequently, the compiled records from tree ring cellulose can only be used to monitor the climate fluctuations of the last millennium at the very best. We have identified ~80 tree ring cellulose $\delta^{18}\text{O}$ records which cover the past 200 years (~80 for $\delta^{13}\text{C}$). Most of the records have been provided at seasonal to decadal temporal resolution.

Lacustrine cores are generally short and records generally span relatively limited time intervals. As a result, only the PD and MH are covered by a relatively large number of records (~35 $\delta^{18}\text{O}$, 30 $\delta^{13}\text{C}$ and ~135 δD records for PD; 25 $\delta^{18}\text{O}$, 30 $\delta^{13}\text{C}$ and ~45 δD records for MH), while datasets spanning the LGM and LIG are very scarce (30 when considering $\delta^{18}\text{O}$, $\delta^{13}\text{C}$ and δD records).

Datasets temporal resolution

Supplementary Fig. A1 (see Appendix) shows the variety of temporal resolutions in the compiled records spanning the past 200 years (1800-2013 CE). Dating of marine sediment core tops remains a critical issue, due to alterations during the coring process as well as sediment reworking and bioturbation. In fact, the upper first centimetres are generally water-soaked and thus often lost or altered during the recovering of marine cores, which, in case of moderate or low sedimentation rates, leads to the loss of material spanning the last hundreds or thousands years. Additionally, bioturbation can alter the upper sediment down to 10 cm below the water-sediment interface (Boudreau, 1998). As a result, many core tops provided as present day references might actually reflect older conditions (from several centuries to few millennia, Barker et al., 2007; Löwemark et al., 2008; Fallet et al., 2012).

Solving these issues might require a precise investigation of bioturbation tracks in the upper layers of sediment cores and drastic improvement of the coring and analysis techniques, as suggested by the final conclusions of Keigwin and Guilderson (2009) : “Until we can directly radiocarbon date individual foraminifera, the role of bioturbation will always be a problem in core top calibration studies”. These sedimentary issues are often accompanied by insufficient resolution and quality of the sediment core-tops dating procedure. In fact, present-day conditions are represented by only one data point in about half of the datasets, generally dated via linear extrapolation of deeper tie-points. About 95 marine $\delta^{18}\text{O}$ and 35 $\delta^{13}\text{C}$ records exhibit a decadal to annual resolution, generally arising from corals (65% of the records) with robust layer-counted annual chronology.

While chronology is not an issue for tree ring cellulose records, the number of individual tree samples combined for each year can be a limiting factor. Several studies have investigated the signal to noise ratio, and demonstrated the importance of combining at least 4-5 trees from a forest to extract the common climate signal (e.g. McCarroll and Loader, 2004; Daux et al., 2011; Labuhn et al., 2014). The same issue arises for ice core records, especially for the past centuries when the noise caused by processes such as wind scouring can be significant when compared to the small climatic signal (e.g. Fisher et al, 1985; Masson-Delmotte et al., 2015). As a result, the records resulting from stacks combining several ice cores from a given site have stronger climatic relevance than records based on individual ice cores. However, the non-polar ice cores experience their best dating on this period. The dating is usually based on the multi-proxy annual layer counting which is based on the seasonal variations of insoluble particles and the isotopic composition of ice. Moreover, the natural radioactive material decay of suitable radionuclides (Pb^{210} for example) and the identification of prominent horizons of known age from radioactive fallout after atmospheric thermonuclear test bombs (Cs^{137} , Sr^{90} , Am^{241}) provide absolute reference horizons, and are currently used in the Southern Hemisphere (Vimeux et al., 2008, 2009a for example in the Andes).

Several recent speleothem and short ice core records benefit from annual layer counting, with an accurate chronology, but this is not systematic. Ice core datasets encompass a large proportion (~70%; 120 records) of highly-resolved (decadal to annual) records, while this percentage is significantly reduced for speleothems (about one half of the 90 records spanning the last 200 years).

For the MH and LGM, marine records also have the lowest temporal resolution, as 80% of these datasets exhibit 4 data points or less over the 5.5-6.5 ka interval, and none of the records are available with a resolution better than respectively 20 and 40 years (Fig. A2 and A3 in Appendix). Ice core records spanning the MH and the LGM are relatively scarce (55 and ~50 datasets, respectively), and most of them exhibit decadal to centennial resolution. Speleothem records are slightly more abundant than ice core records (90 and 55 records for the MH and the LGM, respectively), with very variable resolution, from millennial to sub-decadal. Speleothems and ice core records spanning the Last Interglacial are scarce (about 35 and 15 records, respectively; Fig. A4 in Appendix) and only some of them present a centennial resolution or better, while marine records are abundant, but most of them have millennial or lower temporal resolution.

Lacustrine data can roughly be divided into two groups, with about half of the records covering only the last decades, while the other records are generally much longer, spanning the Holocene period, and few datasets cover the glacial period.

The present day is somewhat well resolved, as about 65 % of the $\delta^{18}\text{O}$ and $\delta^{13}\text{C}$ records spanning this time interval exhibit at least ten data points. This trend is also observed for the MH, with about 65 % of the records presenting ten or more data points. δD records appear to be much less well resolved, mostly because a large number of records originate from surface sediment studies based on dated core tops, resulting in a single data point. As a result, only 20 % on the δD records show at least ten data points for the PD. This lower resolution for δD is also verified for the MH, as none of the records present more than ten data points.

Age model quality evaluation

Results from the evaluation of the quality of chronologies are highly variable from marine and lacustrine cores to speleothems (Fig. 7). The overall quality of age models for marine records is moderate. In fact, we note that most of the records published in the 20th century present a missing or crude age model based on an insufficient number of AMS ^{14}C dates, with a lack of reported technical information. Although this result is somewhat deceiving, the quality of age controls has strongly improved during the last 15 years, thanks to better dating technologies and the

growing awareness of the absolute necessity to publish robust and well detailed chronologies to precisely reconstruct past climate fluctuations.

Age models in speleothems are much better constrained, as most of the records present an “excellent” or “good” quality flag. Speleothem records are indeed generally constrained by abundant U-Th dates and authors often provide highly detailed technical information. Age anomalies such as age reversals, outliers and hiatuses are nevertheless identified in many records. These anomalies can be caused by analytical issues (e.g. sample contamination, Th adsorption; Musgrove et al., 2001; Wainer et al., 2011) or natural factors occurring simultaneously or after sedimentation process (diagenetic alteration). Hiatuses may be induced by climatic (e.g. severe droughts or permafrost impacts) or post-deposition (e.g. carbonate dissolution) factors (Lachniet, 2009; Breitenbach et al., 2012).

The age models of lacustrine records are relatively good overall, with however large discrepancies in the quality of chronologies, depending on the dating technique. In fact, some lacustrine records are dated by counting annual/seasonal varves or laminations, leading to an excellent chronology. This dating technique is however generally limited to relatively short records. Records providing longer signals (i.e. spanning several thousand years) are generally dated by AMS ^{14}C dates. Similarly to what is observed for marine core dating, we note the possible lack of technical information in publications, as well as limited resolution of dates, which prevent the establishment of robust age-models. Also, the potential adjustment applied to ^{14}C ages to correct from radiocarbon reservoir and residence time effects is not systematically provided, as well as the presence of possible hiatuses.

6.2 Changes between PMIP key periods

$\delta^{18}\text{O}$ from oceans and atmospheric water (and therefore continental archives) vary in an opposite directions with climate fluctuations. We thus reversed $\delta^{18}\text{O}$ fluctuations from ocean records in order to map coherent $\delta^{18}\text{O}$ trends from all the different archives. We however report the original values in the text. We report anomalies with respect to the MH for coherency.

6.2.1 Changes between MH and Present-Day

The relatively large number of dated $\delta^{18}\text{O}$ datasets covering both the last 200 years (PD) and the Mid-Holocene (MH) allows us to estimate possible offsets between these two periods (MH-PD; ~100 records from 70 sites; Fig. 8). We restrict the record selection to datasets presenting multiple data points for each of the two periods of interest, thus documenting both the signal (average value) and noise (standard deviation). Results indicate a large dispersion of data, ranging from large positive to negative offsets, while most of the records depict in fact very similar values for the two periods. This feature reflects the spatial heterogeneity of the response to climate changes, making particularly difficult the establishment of large-scale patterns. In a given region, differences also emerge between records from different archives (e.g. opposite sign of changes in speleothem vs lake records in Eastern Europe). The average difference is low in ice cores, but the overall negative offset observed in ice cores indicates a polar cooling during the last 6 ka, except around the Ross Sea in Antarctica. Particularly remarkable is also the positive anomaly from Chinese speleothems, commonly attributed to changes in Asian summer monsoon with a decrease in rainfall amount through the Holocene (Cai et al., 2010). The standard deviation of the data for the two periods of interest are however quite large in most cases. In fact, in the three types of archives, this noise is either of the same order or higher than the calculated PD-MH offset. As a result, the relatively weak isotopic change between these two periods is not significant in 2/3 of the records. Because we did not account the analytical error associated with $\delta^{18}\text{O}$ measurements (as this indication was missing in some of the datasets), we may underestimate the noise level, and thus the number of records presenting an insignificant PD-MH offset.

6.2.2 Changes between the Last interglacial and MH

We now apply the same approach for the change between LIG and MH (Fig. 9). This relies on 75 $\delta^{18}\text{O}$ records from ~45 sites presenting multiple data points for both of the two periods of interest. We observe more enriched continental (more depleted marine) $\delta^{18}\text{O}$ values for LIG than during the MH in ~20 records, suggesting relatively warmer conditions during LIG, with no apparent geographical trend. However, about half of the LIG-MH anomalies are in the range of the natural standard deviation, and thus cannot be considered as statistically significant. Considering only the records presenting a significant offset nevertheless suggests warmer conditions (enriched continental and depleted marine $\delta^{18}\text{O}$) values during the LIG than MH.

Recent syntheses have shown contrasting results in temperature changes between the Last Interglacial period and present day (e.g. Otto-Bliesner et al., 2013), with positive temperature anomalies at both poles, but not occurring simultaneously (Capron et al., 2014), and negative temperature anomalies in some tropical areas. Contrasted regional patterns are expected from the different orbital configurations. Several studies have also highlighted a large magnitude of climate variability during the LIG period (Cheddadi et al., 1998; Lototskaya and Ganssen, 1999; Hearty et al., 2007; Rohling et al., 2007; Pol et al, 2014).

6.2.2 Changes between the LGM and MH

Due to the limited amount of well-dated marine $\delta^{18}\text{O}$ records covering both the LGM and present day with more than one data point, we compare the LGM and the Mid-Holocene for investigating the isotopic amplitude of last termination (Fig. 10). The LGM-MH comparison reveals a significant negative (positive) offset in almost all the terrestrial (marine) records, with only few speleothem and coral records showing the opposite trend, mostly in the subtropics where they may reflect precipitation or atmospheric circulation effects rather than local temperature variations. The highest deglacial amplitude is recorded in high elevation and polar ice core records, while the offset is less marked in oceans and speleothems. Marine datasets reveal a latitude-independent general amplitude of ~1.45 ‰ (1.55 ‰ when

considering only foraminiferal records, with a similar average value for benthics and planktonics), out of which ~1 ‰ is due to the change in land ice volume. In addition, we observe specific regional patterns. Larger amplitudes are identified in marine records from the north and South-East Atlantic (about 1.7 ‰), which contrast with smaller amplitudes in the tropics (~1.5 ‰) and maximum signals in the Mediterranean Sea (about 2.5 ‰). In this basin, this strong isotopic change is understood to reflect large SSTs deglacial warming and salinity changes induced by shifts in the regional atmospheric circulation (Bigg, 1994; Emeis et al., 2000; Hayes et al., 2005; Mikolajewicz, 2011). Statistics based on benthic foraminiferal $\delta^{18}\text{O}$ records (including datasets presenting only one data point in the periods of interest) reveal that there is no influence of core site depth on the amplitude of the LGM to MH transition ($R^2 = 0.0029$; $n = 180$).

Ice cores records from high latitudes are all marked by a -3.3 to -7.7 ‰ $\delta^{18}\text{O}$ shift, with however regional differences such as East-West gradients in both Greenland and Antarctica. Such regional differences may be induced by changes in ice sheet topography and different amplitudes of surface elevation changes at different locations (e.g. Vinther et al., 2009). Similar mechanisms may be at play in Antarctica, but remain poorly documented (e.g. Masson-Delmotte et al., 2011b). There is also evidence for regional differences in the response of Antarctic temperature to climatic changes (Turner et al., 2005; Steig et al., 2009; Steig and Orsi, 2013). The larger amplitude of glacial-interglacial isotopic changes in West Antarctica has been suggested to reflect regional processes coupling the Southern Ocean, sea ice extent and atmospheric heat transport (WAIS Divide Project Members, 2013). It is worth noting that Andean ice cores spanning the last glacial-interglacial transition show a similar deglacial isotopic shift (Vimeux, 2009b). The water stable isotopic composition in those ice cores is likely reflecting precipitation changes at regional scale and such a similar deglacial structure is explained by simultaneous cold conditions in the high latitudes and wetter conditions in the Andes (Vimeux et al., 2005; Chiang and Koutavas, 2008).

Different patterns emerge from speleothem records covering the LGM and MH, as only half of the datasets are marked by a more depleted glacial $\delta^{18}\text{O}$ level. Depending on the location, speleothem calcite $\delta^{18}\text{O}$ may reflect either paleotemperature and/or past changes in atmospheric water cycle (including

precipitation and circulation). Additional site-specific factors (cave microclimate, mixing and evaporation of source waters through the soil and the epikarst, kinetic fractionation during carbonate precipitation) may also influence the signal (Lachniet, 2009). Regional effects may also be at play in the western Middle East, where speleothem records can be directly influenced by changes in the Mediterranean or the Black Sea, which had diverging oceanographic evolutions between the LGM and the MH, with the opening of the Bosphorus Strait. Individual records must therefore be understood in their own regional environmental context, a feature also evidenced by different amplitudes of change arising from different source archives. Thus, Fig. 8-10 might be considered as an inventory of the available datasets, rather than a cartography of the amplitude of climatically-relevant signals, expected to be representative of the amplitude of annual mean precipitation or sea water isotopic composition changes.

7. Conclusions, recommendations and perspectives

Our compilation of hundreds of records from different sources highlights the needs for a standardized protocol of data storage. The output files provided by the different depositories have different archiving formats. Several ongoing projects rely on massive and automated extraction of datasets provided by authors. This effort would be made easier if the data and publication information (core site specifications, references, article title and abstract) were stored in individual CSV (Comma-Separated Values) text files, rather than within files specifically designed for spreadsheet software (e.g. Microsoft Excel/Apache OpenOffice), sometimes containing several spreadsheets, that may not be readable by automated data extraction programs. We also think that building a fixed disposition for datasets constitutes a preliminary step and that it is essential for the existing and future data depositories to find an agreement for an harmonized disposition, structure and labelling for metadata and age modelling data storage. Some projects are following a promising philosophy of homogenously-structured metadata (e.g. LiPD; McKay and Emile-Geay, 2015). We highly encourage these constructive initiatives, as it becomes urgent for the palaeoclimate research community to definitively adopt a universal file format and metadata disposition, and define the type of contents to be included, before starting compiling data, otherwise this will lead to a high risk of incompatibility

or of conflicting information from different sources or projects. Adopting this universal format will however necessitate a clear agreement between data producers, users, and compilers, as it requests at the end a unique structure compatible with all types of archive and proxies, which may lead to some complications due to the variable number of parameters to be included for each proxy and archive. When a universal standard format will be definitively adopted, the conversion of our metadata spreadsheet into a hierarchical structured may be relatively easy and fast.

Divergences in data units also constitute a major obstacle for automated extraction, inter-comparison of records, and model-data comparisons. An illustrative example is the use of various time units (years CE, years or before 2000 CE, years before 1950 CE, kiloyears BP, and million years BP). The establishment of standard time units for palaeoclimatology such as use of ka (calendar kiloyears before 1950) would avoid errors and homogenization of future datasets. Several discrepancies also exist with respect to the geographical coordinates of core sites. Although the most common format found in the literature is DMS (Degrees, Minutes, Seconds; e.g.: 25°22'34"N, 38°16'43"W), it is not supported by most mapping programs. Here, we converted all the geographical coordinates into decimal degrees. We again highly encourage the adoption of a standard notation, with the systematic presence of the decimal degree version of the coordinates; we observe that an increasing number of authors now provide both DMS and decimal formats.

Gathering information about the age models was a particularly critical step of the construction of this database, in particular for the inclusion of lacustrine and deep sea cores as well as speleothems. We highly encourage the authors to systematically provide both depth and age scales as well as a comprehensive description of the methodology used to establish the age scale, when available. While our earlier comment was centered on deep sea cores, the same features apply for the description of lake sediment cores, ice cores and speleothem chronologies. Even if the methodology developed for the successive chronologies of deep ice cores is usually precisely documented, no standardized reporting protocol exists for ice cores from tropical and temperate glaciers. There is however no existing standard procedure for the description of age models. The available information is often fragmented, with missing information (raw AMS ¹⁴C dates, calibration program/curve

used to compute calendar ages, species used for analysis, amount of material measured, marine reservoir ages, tie points, identification of hiatuses in speleothems...). A standardized format including all the information related to the establishment of the age models would be a major step forward. Finding a common structure might however constitute a fastidious task, particularly because the samples dating techniques are radically different for the different types of archives. A first step would constitute in finding a standard structure to be adopted for AMS ^{14}C measurements performed, for instance, on speleothems, marine and lacustrine cores. Many old records are associated to very limited information concerning their chronology, which prevents any tentative to reproduce the age model. Consequently, it becomes necessary to adopt a common format which would be interoperable between the different data repositories, and would include all the necessary information to recalculate age models. For age models based on AMS ^{14}C dating, we suggest that the following information should become mandatory:

- Core ID
- Sample ID, lab name
- Sample depth with indication of any depth correction
- Type of material analysed, including species.
- Indication of sedimentary disturbances (hiatuses, turbidites, tephras, etc...) and their corresponding depth
- AMS ^{14}C ages and the associated error
- Calibrated ages and the associated error
- Program/calibration curve used for ^{14}C dates calibration
- Reservoir age for marine cores, and the associated uncertainties
- Dates removed from the construction of the age model and the reason why they were eliminated.

Additional information might include the type of equipment used for analysis and the date of measurement, the posterior probability distributions of ^{14}C dates, the treatment applied for sample cleaning and the amount (weight or number of specimens) of material analysed.

We have noticed a clear improvement of the quality of age models and of dating techniques description during the last two decades, and most of the low quality chronologies were published more than 20 years ago. This improvement of age models is particularly critical with respect to the sequences of events during fast transient climate reorganizations. In fact, previous studies have shown that many past major climate changes involved abrupt responses (e.g. de Menocal et al., 2000; Genty et al., 2006; Carlson et al., 2007; Zuraida et al., 2009; Clark et al., 2012; Rach et al., 2014) as well as short delays between different proxy records and regions, like the vigorously debated date and triggering of the onset of Termination I (Schaeffer et al., 2006; Stott et al., 2007; Koutavas and Sachs, 2008; Smith et al., 2008; Bromley et al., 2009; Clark et al., 2009; Shakun et al., 2012; Parrenin et al., 2013). In this context of successive rapid climatic events and keeping in mind the growing interest on transient climate simulations, it thus becomes necessary to have a large amount of precisely dated and well defined records. Reservoir ages remain a critical issue in palaeoceanography as well as their uncertainties. Many efforts have been deployed during the last decade to better estimate reservoir ages. Several publications have also suggested changes in reservoir ages between glacial and interglacial periods (e.g. Waelbroeck et al., 2001; Bondvik et al., 2006; Sikes et al., 2016). In this context, the age model of many old records may be outdated, and even considered to be wrong. Unfortunately, the lack of information concerning the construction of these initial age models makes the construction of an updated age model virtually impossible. In this study, we did not aim to evaluate the accuracy of published reservoir ages, which remain sometimes vigorously debated. We encourage authors of publications to systematically justify their choice of a reservoir age, to describe the associated uncertainties, together with the detailed age model information.

Our database may in the future allow the implementation of statistical age models built on the existing age markers. Reporting the exact number of source records for tree rings and ice cores is also important with respect to the signal to noise issue; this is not always a standard practice.

Our software tool was designed to make the update of the database user-friendly and easy, in order to allow future extension. Indeed, major synthesis efforts as the MARGO project (Waelbroeck et al., 2009) are time limited (MARGO only includes

records published prior to 2005). Options for an automatic update include a regular browsing of new published data, but we highly encourage authors to upload their new data in our database using the user-friendly interface on the online platform. This constitutes a fast and easy way to disseminate new data and increase their visibility, and a unique opportunity for the scientific community to access and exploit newly published datasets. This allows “data producers” to easily compare their records with other existing records in a given area or at the global scale, and climate modelers to access easily the data, and to the source references and their authors.

In the future, and if manpower resources are available, the database and web interface could be easily opened to other proxies (paleotemperature proxies and nitrogen isotopes for seawater, CO₂ and CH₄ from ice cores, tree rings width and boreholes, pollens, circulation tracers such as ¹⁴C and Pa/Th, etc.) of past and future datasets. We also hope that our database, associated with current and upcoming projects focusing on time-series age control (INTIMATE PROJECT, COST Action ES0907) and chronological data managing (Mulitza and Paul, in prep.), would in the future facilitate the use of paleoclimate datasets for data comparison and integration into models with an homogenous and robust chronological frame. This is expected to strengthen the use of proxy information for model-data comparisons, a topic promoted in the Stable Water Isotope Intercomparison group (SWING) and the isotope modeling working group of the Paleoclimate Modelling Intercomparison project, with the potential to better document projections (Schmidt et al, 2014).

Acknowledgements

This study was supported by a national grant from the Agence Nationale de la Recherche under the “Programme d'Investissements d'Avenir” (Grant #ANR-10-LABX-0018) within the framework of LABEX L-IPSL.

References

- Ahagon, N., Ohkushi, K., Uchida, M., and Mishima, T.: Mid-depth circulation in the northwest Pacific during the last deglaciation: Evidence from foraminiferal radiocarbon ages, *Geophys. Res. Lett.*, 30, 2097, 2.1-2.4, doi:10.1029/2003GL018287, 2003.
- Araguas-Araguas, L., Froehlich, K., and Rozanski, K.: Deuterium and oxygen-18 isotope composition of precipitation and atmospheric moisture, *Hydrological Processes*, 14, 1341-1355, 10.1002/1099-1085(20000615)14:8<1341::aid-hyp983>3.0.co;2-z, 2000.
- Bakker, P., Masson-Delmotte, V., Martrat, B., Charbit, S., Renssen, H., Gröger, M., Krebs-Kanzow, U., Lohmann, G., Lunt, D. J., Pfeiffer, M., Phipps, S. J., Prange, M., Ritz, S. P., Schulz, M., Stenni, B., Stone, E. J., and Varma, V.: Temperature trends during the Present and Last Interglacial periods – a multi-model-data comparison, *Quaternary Science Reviews*, 99, 224-243, 10.1016/j.quascirev.2014.06.031, 2014.
- Bard, E.: Radiocarbon Calibration/Comparison Records Based on Marine Sediments from the Pakistan and Iberian Margins, *Radiocarbon*, 55, 1999-2019, 10.2458/azu_js_rc.55.17114, 2013.
- Barker, S., Broecker, W., Clark, E., and Hajdas, I.: Radiocarbon age offsets of foraminifera resulting from differential dissolution and fragmentation within the sedimentary bioturbated zone, *Paleoceanography*, 22, PA2205, doi:10.1029/2006pa001354, 2007.
- Bar-Matthews, M., Ayalon, A., Gilmour, M., Matthews, A., and Hawkesworth, C. J.: Sea-land oxygen isotopic relationships from planktonic foraminifera and speleothems in the Eastern Mediterranean region and their implication for paleorainfall during interglacial intervals, *Geochimica et Cosmochimica Acta*, 67, 3181-3199, 10.1016/s0016-7037(02)01031-1, 2003.

1020 Bazin, L., Landais, A., Lemieux-Dudon, B., Toyé Mahamadou Kele, H., Veres, D.,
 1021 Parrenin, F., Martinerie, P., Ritz, C., Capron, E., Lipenkov, V., Loutre, M. F.,
 1022 Raynaud, D., Vinther, B., Svensson, A., Rasmussen, S. O., Severi, M., Blunier, T.,
 1023 Leuenberger, M., Fischer, H., Masson-Delmotte, V., Chappellaz, J., and Wolff, E.: An
 1024 optimized multi-proxy, multi-site Antarctic ice and gas orbital chronology (AICC2012):
 1025 120–800 ka, *Climate of the Past*, 9, 1715-1731, 10.5194/cp-9-1715-2013,
 1026 2013.

1027

1028 Berger, W. H., and Winterer, E. L., : Plate stratigraphy and fluctuating carbonate line.
 1029 In Hsü, K. J., and Jenkyns, H. C. (eds.), *Pelagic Sediments on Land and Under the*
 1030 *Sea*. Oxford: International Association of Sedimentologists Special Publication, Vol.
 1031 1, 11–48, doi: 10.1002/9781444304855.ch2, 1974.

1032

1033 Bigg, G. R.: An ocean general circulation model view of the glacial Mediterranean
 1034 thermohaline circulation, *Paleoceanography*, 9, 705-722, 10.1029/94pa01183, 1994.

1035

1036 Blockley, S. P. E., Lane, C. S., Hardiman, M., Rasmussen, S. O., Seierstad, I.,
 1037 Steffensen, J. P., Svensson, A., Lotter, A. F., Turney, C. S. M., Ramsey, C. B. &
 1038 INTIMATE members: Synchronisation of palaeoenvironmental records over the last
 1039 60,000 years, and an extended INTIMATE event stratigraphy to 48,000 b2k.
 1040 *Quaternary Science Reviews* 36, 2–10 10.1016/j.quascirev.2011.09.017, 2012.

1041

1042 Bolliet, T., Holbourn, A., Kuhnt, W., Laj, C., Kissel, C., Beaufort, L., Kienast, M.,
 1043 Andersen, N., and Garbe-Schönberg, D.: Mindanao Dome variability over the last
 1044 160 kyr: episodic glacial cooling of the West Pacific Warm Pool, *Paleoceanography*,
 1045 26, PA1208, doi:10.1029/2010pa001966, 2011.

1046

1047 Bondevik, S., Mangerud, J., Birks, H. H., Gulliksen, S., and Reimer, P.: Changes in
 1048 North Atlantic Radiocarbon Reservoir Ages During the Allerød and Younger Dryas,
 1049 *Science*, 312, 1514–1517, doi: 10.1126/science.1123300, 2006.

1050

1051 Boudreau, B. P.: Mean mixed depth of sediments: The wherefore and the why,
 1052 *Limnology and Oceanography*, 43, 524-526, 10.4319/lo.1998.43.3.0524, 1998.

1053

1054 Bouttes, N., Paillard, D., Roche, D. M., Waelbroeck, C., Kageyama, M., Laurantou,
 1055 A., Michel, E., and Bopp, L.: Impact of oceanic processes on the carbon cycle during
 1056 the last termination, *Climate of the Past*, 8, 149-170, 10.5194/cp-8-149-2012, 2012.

1057

1058 Braconnot, P., Harrison, S. P., Kageyama, M., Bartlein, P. J., Masson-Delmotte, V.,
 1059 AbeOuchi, A., Otto-Bliesner, B., and Zhao, Y.: Evaluation of climate models using
 1060 palaeoclimatic data, *Nature Clim. Change*, 2, 417–424, doi:10.1038/nclimate1456,
 1061 2012.

1062

1063 Braconnot, P.: Mid-Holocene and Last Glacial Maximum African monsoon changes
 1064 as simulated within the Paleoclimate Modelling Intercomparison Project, *Global and*
 1065 *Planetary Change*, 26, 51-66, 10.1016/s0921-8181(00)00033-3, 2000.

1066

1067 Breitenbach, S. F. M., Rehfeld, K., Goswami, B., Baldini, J. U. L., Ridley, H. E.,
 1068 Kennett, D. J., Prufer, K. M., Aquino, V. V., Asmerom, Y., Polyak, V. J., Cheng, H.,
 1069 Kurths, J., and Marwan, N.: COConstructing Proxy Records from Age models (COPRA),
 1070 *Climate of the Past*, 8, 1765-1779, 10.5194/cp-8-1765-2012, 2012.

1071

1072 Broccoli, A. J., Dahl, K. A., and Stouffer, R. J.: Response of the ITCZ to Northern
 1073 Hemisphere cooling, *Geophys. Res. Lett.*, 33, L01702, doi:10.1029/2005gl024546,
 1074 2006.

1075

1076 Bromley, G. R. M., Schaefer, J. M., Winckler, G., Hall, B. L., Todd, C. E., and
 1077 Rademaker, K. M.: Relative timing of last glacial maximum and late-glacial events in
 1078 the central tropical Andes, *Quaternary Science Reviews*, 28, 2514-2526,
 1079 10.1016/j.quascirev.2009.05.012, 2009.

1080

1081 Bronk Ramsey, C., Scott, E.M. and van der Plicht, J.: Calibration For Archaeological
 1082 And Environmental Terrestrial Samples In The Time Range 26–50 Ka Cal Bp,
 1083 *Radiocarbon*, 55 (4),2021-2027, 2013.

1084

Buizert, C., Gkinis, V., Severinghaus, J. P., He, F., Lecavalier, B. S., Kindler, P.,
Leuenberger, M., Carlson, A. E., Vinther, B., Masson-Delmotte, V., White, J. W. C.,
Liu, Z., Otto-Bliesner, B., and Brook, E. J.: Greenland temperature response to
climate forcing during the last deglaciation, *Science*, 345, 1177-1180,
10.1126/science.1254961, 2014.

Burke, A., and Robinson, L. F.: The Southern Ocean's Role in Carbon Exchange
During the Last Deglaciation, *Science*, 335, 557-561, 10.1126/science.1208163,
2011.

Cai, Y., Tan, L., Cheng, H., An, Z., Edwards, R., Kelly, M., Kong, X., and Wang, X.:
The variation of summer monsoon precipitation in central China since the last
deglaciation, *Earth Planet. Sci. Lett.*, 291, 21–31, 2010

Caley, T. and Roche, D. M.: $\delta^{18}\text{O}$ water isotope in the iLOVECLIM model (version
1.0) – Part 3: A palaeo-perspective based on present-day data–model comparison for
oxygen stable isotopes in carbonates, *Geosci. Model Dev.*, 6, 1505-1516,
doi:10.5194/gmd-6-1505-2013, 2013.

Caley, T., Roche, D. M., Waelbroeck, C., and Michel, E.: Oxygen stable isotopes
during the Last Glacial Maximum climate: perspectives from data–model
iLOVECLIM) comparison, *Climate of the Past*, 10, 1939-1955, 10.5194/cp-10-1939-
2014, 2014.

Capron E., Govin A., Stone E. J., Masson-Delmotte V., Mulitza S., Otto-Bliesner B.,
Rasmussen T. L., Sime L. C., Waelbroeck C., and Wolff E. W.: Temporal and spatial
structure of multi-millennial temperature changes at high latitudes during the Last
Interglacial. *Quaternary Science Reviews*, 103, 116-133.
10.1016/j.quascirev.2014.08.018, 2014.

Carlson, A. E., Clark, P. U., Raisbeck, G. M., and Brook, E. J.: Rapid Holocene
Deglaciation of the Labrador Sector of the Laurentide Ice Sheet, *Journal of Climate*,
20, 5126-5133, 10.1175/jcli4273.1, 2007.

Carré, M., Azzoug, M., Bentaleb, I., Chase, B. M., Fontugne, M., Jackson, D., Ledru, M.-P., Maldonado, A., Sachs, J. P., and Schauer, A. J.: Mid-Holocene mean climate in the south eastern Pacific and its influence on South America, *Quaternary International*, 253, 55-66, 10.1016/j.quaint.2011.02.004, 2012.

Cheddadi, R., Lamb, H. F., Guiot, J., and van der Kaars, S.: Holocene climatic change in Morocco: a quantitative reconstruction from pollen data, *Climate Dynamics*, 14, 883-890, 10.1007/s003820050262, 1998.

Chiang J.C.H. and Koutavas A., Climate change: tropical flip-flop connections, *Nature* 432 (7018), 684-685, 2004.

Chylek, P., Lesins, G., and Lohmann, U.: Enhancement of dust source area during past glacial periods due to changes of the Hadley circulation, *Journal of Geophysical Research*, 106, 18477, 10.1029/2000jd900583, 2001.

Clark, C. D., Hughes, A. L. C., Greenwood, S. L., Jordan, C., and Sejrup, H. P.: Pattern and timing of retreat of the last British-Irish Ice Sheet, *Quaternary Science Reviews*, 44, 112-146, 10.1016/j.quascirev.2010.07.019, 2012.

Clark, P. U., Dyke, A. S., Shakun, J. D., Carlson, A. E., Clark, J., Wohlfarth, B., Mitrovica, J. X., Hostetler, S. W., and McCabe, A. M.: The Last Glacial Maximum, *Science*, 325, 710-714, 10.1126/science.1172873, 2009.

Collins, M., R. Knutti, J. Arblaster, J.-L. Dufresne, T. Fichet, P. Friedlingstein, X. Gao, W.J. Gutowski, T. Johns, G. Krinner, M. Shongwe, C. Tebaldi, A.J.Weaver and M. Wehner : Long-term Climate Change: Projections, Commitments and Irreversibility. In: *Climate Change 2013: The Physical Science Basis. Contribution of Working Group I to the Fifth Assessment Report of the Intergovernmental Panel on Climate Change* [Stocker, T.F., D. Qin, G.-K.Plattner, M. Tignor, S.K. Allen, J. Boschung, A. Nauels, Y. Xia, V. Bex and P.M. Midgley (eds.)]. Cambridge University Press, Cambridge, United Kingdom and New York, NY, USA, pp. 1029–1136, doi:10.1017/CBO9781107415324.024, 2013.

1153 Cruz, F. W., Burns, S. J., Karmann, I., Sharp, W. D., and Vuille, M.: Reconstruction of
 1154 regional atmospheric circulation features during the late Pleistocene in subtropical
 1155 Brazil from oxygen isotope composition of speleothems, *Earth and Planetary Science*
 1156 *Letters*, 248, 495-507, 10.1016/j.epsl.2006.06.019, 2006.

1157

1158 Csank, A. Z.: An International Tree-Ring Isotope Data Bank– A Proposed Repository
 1159 for Tree-Ring Isotopic Data. *Tree-Ring Research*, 65(2), 163–164. doi:10.3959/1536-
 1160 1098-65.2.163, 2009.

1161 Dahl-Jensen, D., Albert, M. R., Aldahan, A., Azuma, N., Balslev-Clausen, D.,
 1162 Baumgartner, M., Berggren, A. M., Bigler, M., Binder, T., Blunier, T., Bourgeois, J. C.,
 1163 Brook, E. J., Buchardt, S. L., Buizert, C., Capron, E., Chappellaz, J., Chung, J.,
 1164 Clausen, H. B., Cvijanovic, I., Davies, S. M., Ditlevsen, P., Eicher, O., Fischer, H.,
 1165 Fisher, D. A., Fleet, L. G., Gfeller, G., Gkinis, V., Gogineni, S., Goto-Azuma, K.,
 1166 Grinsted, A., Gudlaugsdottir, H., Guillevic, M., Hansen, S. B., Hansson, M.,
 1167 Hirabayashi, M., Hong, S., Hur, S. D., Huybrechts, P., Hvidberg, C. S., Iizuka, Y.,
 1168 Jenk, T., Johnsen, S. J., Jones, T. R., Jouzel, J., Karlsson, N. B., Kawamura, K.,
 1169 Keegan, K., Kettner, E., Kipfstuhl, S., Kjær, H. A., Koutnik, M., Kuramoto, T., Köhler,
 1170 P., Laepple, T., Landais, A., Langen, P. L., Larsen, L. B., Leuenberger, D.,
 1171 Leuenberger, M., Leuschen, C., Li, J., Lipenkov, V., Martinerie, P., Maselli, O. J.,
 1172 Masson-Delmotte, V., McConnell, J. R., Miller, H., Mini, O., Miyamoto, A., Montagnat-
 1173 Rentier, M., Mulvaney, R., Muscheler, R., Orsi, A. J., Paden, J., Panton, C., Pattyn,
 1174 F., Petit, J. R., Pol, K., Popp, T., Possnert, G., Prié, F., Prokopiou, M., Quiquet, A.,
 1175 Rasmussen, S. O., Raynaud, D., Ren, J., Reutenauer, C., Ritz, C., Röckmann, T.,
 1176 Rosen, J. L., Rubino, M., Rybak, O., Samyn, D., Sapart, C. J., Schilt, A., Schmidt, A.
 1177 M. Z., Schwander, J., Schüpbach, S., Seierstad, I., Severinghaus, J. P., Sheldon, S.,
 1178 Simonsen, S. B., Sjolte, J., Solgaard, A. M., Sowers, T., Sperlich, P., Steen-Larsen,
 1179 H. C., Steffen, K., Steffensen, J. P., Steinhage, D., Stocker, T. F., Stowasser, C.,
 1180 Sturevik, A. S., Sturges, W. T., Sveinbjörnsdottir, A., Svensson, A., Tison, J. L.,
 1181 Uetake, J., Vallelonga, P., van de Wal, R. S. W., van der Wel, G., Vaughn, B. H.,
 1182 Vinther, B., Waddington, E., Wegner, A., Weikusat, I., White, J. W. C., Wilhelms, F.,
 1183 Winstrup, M., Witrant, E., Wolff, E. W., Xiao, C., and Zheng, J.: Eemian interglacial
 1184 reconstructed from a Greenland folded ice core, *Nature*, 493, 489-494,
 1185 10.1038/nature11789, 2013.

1186

1187 Daux, V., Edouard, J. L., Masson-Delmotte, V., Stievenard, M., Hoffmann, G., Pierre,
 1188 M., Mestre, O., Danis, P. A., Guibal, F.: Can climate variations be inferred from tree-
 1189 ring parameters and stable isotopes from *Larix decidua*? Juvenile effects, budmoth
 1190 outbreaks, and divergence issue, *Earth Planet. Sc. Lett.*, 309, 221–233,
 1191 doi:10.1016/j.epsl.2011.07.003, 2011.

1192 Dee, S., D. Noone, N. Buening, J. Emile-Geay, and Y. Zhou (2015), SPEEDY-IER:
 1193 A fast atmospheric GCM with water isotope physics, *J. Geophys. Res. Atmos.*, 120,
 1194 73–91, doi:10.1002/2014JD022194.

1195

1196 deMenocal, P., Ortiz, J., Guilderson, T., Adkins, J., Sarnthein, M., Baker, L., and
 1197 Yarusinsky, M.: Abrupt onset and termination of the African Humid Period,
 1198 *Quaternary Science Reviews*, 19, 347-361, 10.1016/s0277-3791(99)00081-5, 2000.

1199 Duplessy, J. C., N. J. Shackleton, R. G. Fairbanks, L. Labeyrie, D. Oppo, and N.
 1200 Kallel, Deepwater source variations during the last climatic cycle and their impact on
 1201 the global deepwater circulation, *Paleoceanography*, 3, 343–360, 1988.

1202

1203 Ehleringer, J.R., and J.C. Vogel: Historical aspects of stable isotopes in plant carbon
 1204 and water relations, p. 9-18. In J.R. Ehleringer, A.E. Hall, and G.D. Farquhar (eds.),
 1205 *Stable Isotopes and Plant Carbon/Water Relations*. Academic Press, San Diego,
 1206 1993.

1207

1208 Emeis, K.-C., Struck, U., Schulz, H.-M., Rosenberg, R., Bernasconi, S., Erlenkeuser,
 1209 H., Sakamoto, T., and Martinez-Ruiz, F.: Temperature and salinity variations of
 1210 Mediterranean Sea surface waters over the last 16,000 years from records of
 1211 planktonic stable oxygen isotopes and alkenone unsaturation ratios,
 1212 *Palaeogeography, Palaeoclimatology, Palaeoecology*, 158, 259-280, 10.1016/s0031-
 1213 0182(00)00053-5, 2000.

1214

1215 Fallet, U., Castañeda, I. S., Henry-Edwards, A., Richter, T. O., Boer, W., Schouten,
 1216 S., and Brummer, G.-J.: Sedimentation and burial of organic and inorganic
 1217 temperature proxies in the Mozambique Channel, SW Indian Ocean, *Deep Sea*
 1218 *Research Part I: Oceanographic Research Papers*, 59, 37-53,
 1219 10.1016/j.dsr.2011.10.002, 2012.

1220

1221 Fisher D. A.: Stratigraphic noise in time series derives from ice cores. *Annals of*
 1222 *Glaciology*, 7, 76-83, 1985.

1223

1224 Flato, G., J. Marotzke, B. Abiodun, P. Braconnot, S.C. Chou, W. Collins, P. Cox, F.
 1225 Driouech, S. Emori, V. Eyring, C. Forest, P. Gleckler, E. Guilyardi, C.Jakob, V.
 1226 Kattsov, C. Reason and M. Rummukainen: Evaluation of Climate Models. In: Climate
 1227 Change 2013: The Physical Science Basis. Contribution of Working Group I to the
 1228 Fifth Assessment Report of the Intergovernmental Panel on Climate Change
 1229 [Stocker, T.F., D. Qin, G.-K. Plattner, M. Tignor, S.K. Allen, J. Boschung, A. Nauels,
 1230 Y. Xia, V. Bex and P.M. Midgley (eds.)]. Cambridge University Press, Cambridge,
 1231 United Kingdom and New York, NY, USA, pp. 741–866,
 1232 doi:10.1017/CBO9781107415324.020, 2013.

1233

1234 Fudge, T. J., Steig, E. J., Markle, B. R., Schoenemann, S. W., Ding, Q., Taylor, K. C.,
 1235 McConnell, J. R., Brook, E. J., Sowers, T., White, J. W. C., Alley, R. B., Cheng, H.,
 1236 Clow, G. D., Cole-Dai, J., Conway, H., Cuffey, K. M., Edwards, J. S., Lawrence
 1237 Edwards, R., Edwards, R., Fegyveresi, J. M., Ferris, D., Fitzpatrick, J. J., Johnson, J.,
 1238 Hargreaves, G., Lee, J. E., Maselli, O. J., Mason, W., McGwire, K. C., Mitchell, L. E.,
 1239 Mortensen, N., Neff, P., Orsi, A. J., Popp, T. J., Schauer, A. J., Severinghaus, J. P.,
 1240 Sigl, M., Spencer, M. K., Vaughn, B. H., Voigt, D. E., Waddington, E. D., Wang, X.,
 1241 and Wong, G. J.: Onset of deglacial warming in West Antarctica driven by local
 1242 orbital forcing, *Nature*, 500, 440-444, 10.1038/nature12376, 2013.

1243

1244 Genty, D., Blamart, D., Ghaleb, B., Plagnes, V., Causse, C., Bakalowicz, M., Zouari,
 1245 K., Chkir, N., Hellstrom, J., and Wainer, K.: Timing and dynamics of the last
 1246 deglaciation from European and North African $\delta^{13}\text{C}$ stalagmite profiles—comparison
 1247 with Chinese and South Hemisphere stalagmites, *Quaternary Science Reviews*, 25,
 1248 2118-2142, 10.1016/j.quascirev.2006.01.030, 2006.

1249

1250 Govin, A., Braconnot, P., Capron, E., Cortijo, E., Duplessy, J.-C., Jansen, E.,
 1251 Labeyrie, L., Landais, A., Marti, O., Michel, E., Mosquet, E., Risebrobakken, B.,
 1252 Swingedouw, D., and Waelbroeck, C.: Persistent influence of ice sheet melting on

1253 high northern latitude climate during the early Last Interglacial, *Clim. Past*, 8, 483-
1254 507, doi:10.5194/cp-8-483-2012, 2012.

1255

1256 Grant, K. M., Rohling, E. J., Bar-Matthews, M., Ayalon, A., Medina-Elizalde, M.,
1257 Ramsey, C. B., Satow, C., and Roberts, A. P.: Rapid coupling between ice volume
1258 and polar temperature over the past 150,000 years, *Nature*, 491, 744–747,
1259 doi:10.1038/nature11593, 2012.

1260

1261 Grant, K. M., Rohling, E. J., Ramsey, C. B., Cheng, H., Edwards, R. L., Florindo, F.,
1262 Heslop, D., Marra, F., Roberts, A. P., Tamisiea, M. E., and Williams, F.: Sea-level
1263 variability over five glacial cycles, *Nat. Commun.*, 5, 5076, doi:10.1038/ncomms6076,
1264 2014.

1265

1266 Guillevic, M., Bazin, L., Landais, A., Kindler, P., Orsi, A., Masson-Delmotte, V.,
1267 Blunier, T., Buchardt, S. L., Capron, E., Leuenberger, M., Martinerie, P., Prié, F., and
1268 Vinther, B. M.: Spatial gradients of temperature, accumulation and $\delta^{18}\text{O}$ -ice in
1269 Greenland over a series of Dansgaard–Oeschger events, *Clim. Past*, 9, 1029-1051,
1270 doi:10.5194/cp-9-1029-2013, 2013.

1271

1272 Harrison, S. P., Bartlein, P. J., Brewer, S., Prentice, I. C., Boyd, M., Hessler, I.,
1273 Holmgren, K., Izumi, K., and Willis, K.: Climate model benchmarking with glacial and
1274 mid-Holocene climates, *Climate Dynamics*, 43, 671-688, 10.1007/s00382-013-1922-
1275 6, 2013.

1276

1277 Hayes, A., Kucera, M., Kallel, N., Sbaifi, L., and Rohling, E. J.: Glacial Mediterranean
1278 sea surface temperatures based on planktonic foraminiferal assemblages,
1279 *Quaternary Science Reviews*, 24, 999-1016, 10.1016/j.quascirev.2004.02.018, 2005.

1280 Hearty, P. J., Hollin, J. T., Neumann, A. C., O’Leary, M. J., and McCulloch, M.: Global
1281 sea-level fluctuations during the Last Interglaciation (MIS 5e), *Quaternary Science*
1282 *Reviews*, 26, 2090-2112, 10.1016/j.quascirev.2007.06.019, 2007.

1283

1284 Henderson-Sellers, A., Fischer, M., Aleinov, I., McGuffie, K., Riley, W. J., Schmidt, G.
1285 A., Sturm, K., Yoshimura, K., and Irannejad, P.: Stable water isotope simulation by

current land-surface schemes: Results of iPILPS Phase 1, Global and Planetary Change, 51, 34-58, 10.1016/j.gloplacha.2006.01.003, 2006.

Hughen, K., Southon, J., Lehman, S., Bertrand, C., and Turnbull, J.: Marine-derived ^{14}C calibration and activity record for the past 50,000 years updated from the Cariaco Basin, Quaternary Science Reviews, 25, 3216-3227, 10.1016/j.quascirev.2006.03.014, 2006.

IAEA/WMO (2015). Global Network of Isotopes in Precipitation. The GNIP Database. Accessible at: <http://www.iaea.org/water> (last access: July 2015), 2015.

IPCC: *Climate Change 2013: The Physical Science Basis. Contribution of Working Group I to the Fifth Assessment Report of the Intergovernmental Panel on Climate Change* [Stocker, T.F., D. Qin, G.-K. Plattner, M. Tignor, S.K. Allen, J. Boschung, A. Nauels, Y. Xia, V. Bex and P.M. Midgley (eds.)]. Cambridge University Press, Cambridge, United Kingdom and New York, NY, USA, 1535 pp, doi:10.1017/CBO9781107415324, 2013.

Jasechko, S., Lechler, A., Pausata, F. S. R., Fawcett, P. J., Gleeson, T., Cendón, D. I., Galewsky, J., LeGrande, A. N., Risi, C., Sharp, Z. D., Welker, J. M., Werner, M., and Yoshimura, K.: Glacial–interglacial shifts in global and regional precipitation $\delta^{18}\text{O}$, Clim. Past Discuss., 11, 831-872, doi:10.5194/cpd-11-831-2015, 2015.

Joussaume, S., Sadourny, R., and Jouzel, J.: A general circulation model of water isotope cycles in the atmosphere, Nature, 311, 24-29, 10.1038/311024a0, 1984.

Justino, F. and Peltier, W. R.: The glacial North Atlantic Oscillation, Geophys. Res. Lett., 32, L21803, doi:10.1029/2005gl023822, 2005.

Keigwin, L. D. and Guilderson, T. P.: Bioturbation artifacts in zero-age sediments, Paleoceanography, 24, PA4212, doi:10.1029/2008pa001727, 2009.

1319 Kohfeld, K. E., and Chase, Z.: Controls on deglacial changes in biogenic fluxes in the
1320 North Pacific Ocean, *Quaternary Science Reviews*, 30, 3350-3363,
1321 10.1016/j.quascirev.2011.08.007, 2011.

1322

1323 Koutavas, A. and Sachs, J. P.: Northern timing of deglaciation in the eastern
1324 equatorial Pacific from alkenone paleothermometry, *Paleoceanography*, 23, PA4205,
1325 doi:10.1029/2008pa001593, 2008.

1326

1327 Kukla, G. J., Bender, M. L., Beaulieu, J.-L. de, Bond, G., Broecker, W. S., Cleveringa,
1328 P., Gavin, J. E., Herbert, T. D., Imbrie, J., Jouzel, J., Keigwin, L. D., Knudsen, K.-L.,
1329 McManus, J. F., Merkt, J., Muhs, D. R., Müller, H., Poore, R. Z., Porter, S., Seret, G.,
1330 Shakleton, N. J., Turner, C. and Winograd, I. J. : Last Interglacial Climates, *Quat.*
1331 *Res.*, 58, 2–13, doi:10.1006/qres.2001.2316, 2002.

1332 Labuhn, I., Daux, V., Pierre, M., Stievenard, M., Girardclos, O., Féron, A., Genty, D.,
1333 Masson-Delmotte, V., and Mestre, O.: Tree age, site and climate controls on tree ring
1334 cellulose $\delta^{18}\text{O}$: A case study on oak trees from south-western France,
1335 *Dendrochronologia*, 32, 78-89, 10.1016/j.dendro.2013.11.001, 2014.

1336

1337 Lachniet, M. S.: Climatic and environmental controls on speleothem oxygen-isotope
1338 values, *Quaternary Science Reviews*, 28, 412-432, 10.1016/j.quascirev.2008.10.021,
1339 2009.

1340

1341 Leduc, G., Vidal, L., Tachikawa, K., and Bard, E.: ITCZ rather than ENSO signature
1342 for abrupt climate changes across the tropical Pacific?, *Quaternary Research*, 72,
1343 123-131, 10.1016/j.yqres.2009.03.006, 2009.

1344

1345 Lee, J.-E., C. Risi, I. Fung, J. Worden, R. A. Scheepmaker, B. Lintner, and C.
1346 Frankenber: Asian monsoon hydrometeorology from TES and SCIAMACHY water
1347 vapor isotope measurements and LMDZ simulations: Implications for speleothem
1348 climate record interpretation, *J. Geophys. Res.*, 117, D15112,
1349 doi:10.1029/2011JD017133, 2012.

1350

1351 Libby, L. M., and Pandolfi, L. J.: Isotopic tree thermometers: Correlation with
 1352 radiocarbon, *Journal of Geophysical Research*, 81, 6377-6381,
 1353 10.1029/JC081i036p06377, 1976.
 1354
 1355 Long, A. 1982. Stable isotopes in tree rings; in *Climate from tree rings* (eds) M. K.
 1356 Hughes, P. M. Kelly, J. R. Pilcher and V. C. LaMarche (Cambridge: Cambridge
 1357 University Press) pp 13–18.
 1358
 1359 Lototskaya, A., and Ganssen, G. M.: The structure of Termination II (penultimate
 1360 deglaciation and Eemian) in the North Atlantic, *Quaternary Science Reviews*, 18,
 1361 1641-1654, 10.1016/s0277-3791(99)00011-6, 1999.
 1362
 1363 Lunt, D. J., Abe-Ouchi, A., Bakker, P., Berger, A., Braconnot, P., Charbit, S., Fischer,
 1364 N., Herold, N., Jungclaus, J. H., Khon, V. C., Krebs-Kanzow, U., Langebroek, P. M.,
 1365 Lohmann, G., Nisancioglu, K. H., Otto-Bliesner, B. L., Park, W., Pfeiffer, M., Phipps,
 1366 S. J., Prange, M., Rachmayani, R., Renssen, H., Rosenbloom, N., Schneider, B.,
 1367 Stone, E. J., Takahashi, K., Wei, W., Yin, Q., and Zhang, Z. S.: A multi-model
 1368 assessment of last interglacial temperatures, *Climate of the Past*, 9, 699-717,
 1369 10.5194/cp-9-699-2013, 2013.
 1370
 1371 Lwemark, L., Jakobsson, M., Mrth, M., and Backman, J.: Arctic Ocean manganese
 1372 contents and sediment colour cycles, *Polar Research*, 27, 105-113, 10.1111/j.1751-
 1373 8369.2008.00055.x, 2008.
 1374
 1375 Marcott, S. A., Shakun, J. D., Clark, P. U., and Mix, A. C.: A Reconstruction of
 1376 Regional and Global Temperature for the Past 11,300 Years, *Science*, 339, 1198-
 1377 1201, 10.1126/science.1228026, 2013.
 1378
 1379 Masson-Delmotte, V., Steen-Larsen, H. C., Ortega, P., Swingedouw, D., Popp, T.,
 1380 Vinther, B. M., Oerter, H., Sveinbjornsdottir, A. E., Gudlaugsdottir, H., Box, J. E.,
 1381 Falourd, S., Fettweis, X., Gallée, H., Garnier, E., Gkinis, V., Jouzel, J., Landais, A.,
 1382 Minster, B., Paradis, N., Orsi, A., Risi, C., Werner, M., and White, J. W. C.: Recent
 1383 changes in north-west Greenland climate documented by NEEM shallow ice core

data and simulations, and implications for past-temperature reconstructions, *The Cryosphere*, 9, 1481-1504, doi:10.5194/tc-9-1481-2015, 2015.

Masson-Delmotte, V., Braconnot, P., Hoffmann, G., Jouzel, J., Kageyama, M., Landais, A., Lejeune, Q., Risi, C., Sime, L., Sjolte, J., Swingedouw, D., and Vinther, B.: Sensitivity of interglacial Greenland temperature and $\delta^{18}\text{O}$: ice core data, orbital and increased CO_2 climate simulations, *Climate of the Past*, 7, 1041-1059, 10.5194/cp-7-1041-2011, 2011a.

Masson-Delmotte, V., Buiron, D., Ekaykin, A., Frezzotti, M., Gallée, H., Jouzel, J., Krinner, G., Landais, A., Motoyama, H., Oerter, H., Pol, K., Pollard, D., Ritz, C., Schlosser, E., Sime, L. C., Sodemann, H., Stenni, B., Uemura, R., and Vimeux, F.: A comparison of the present and last interglacial periods in six Antarctic ice cores, *Clim. Past*, 7, 397-423, doi:10.5194/cp-7-397-2011, 2011b.

Masson-Delmotte, V., Schulz, M., Abe-Ouchi, A., Beer, J., Ganopolski, J., González Rouco, J. F., Jansen, E., Lambeck, K., Luterbacher, J., Naish, T., Osborn, T., OttoBliesner, B., Quinn, T., Ramesh, R., Rojas, M., Shao, X., and Timmermann, A.: Information from paleoclimate archives, in: *Climate Change 2013: The Physical Science Basis. 5 Contribution of Working Group I to the Fifth Assessment Report of the Intergovernmental Panel on Climate Change*, edited by: Stocker, T. F., Qin, D., Plattner, G.-K., Tignor, M., Allen, S. K., Doschung, J., Nauels, A., Xia, Y., Bex, V., and Midgley, P. M., Cambridge University Press, Cambridge, U.K., 383–464, doi:10.1017/CBO9781107415324.013, 2013.

Max, L., Lembke-Jene, L., Riethdorf, J. R., Tiedemann, R., Nürnberg, D., Kühn, H., and Mackensen, A.: Pulses of enhanced North Pacific Intermediate Water ventilation from the Okhotsk Sea and Bering Sea during the last deglaciation, *Climate of the Past*, 10, 591-605, 10.5194/cp-10-591-2014, 2014.

Masson-Delmotte, V., Stenni, B., Blunier, T., Cattani, O., Chappellaz, J., Cheng, H., Dreyfus, G., Edwards, R. L., Falourd, S., Govin, A., Kawamura, K., Johnsen, S. J., Jouzel, J., Landais, A., Lemieux-Dudon, B., Laurantou, A., Marshall, G., Minster, B.,

Mudelsee, M., Pol, K., Rothlisberger, R., Selmo, E., and Waelbroeck, C.: Abrupt change of Antarctic moisture origin at the end of Termination II, Proceedings of the National Academy of Sciences, 107, 12091-12094, 10.1073/pnas.0914536107, 2010.

McCarroll, D. and Loader, N. J.: Stable isotopes in tree rings, Quaternary Sci. Rev., 23, 771– 801, doi:10.1016/j.quascirev.2003.06.017, 2004.

McKay, N. P., and J. Emile-Geay (2015), Technical note: The linked paleo data framework: a common tongue for paleoclimatology, Climate of the Past Discussions, 11(5), 4309–4327, doi:10.5194/cpd-11-4309-2015.

Menviel, L., Joos, F., and Ritz, S. P.: Simulating atmospheric CO₂, ¹³C and the marine carbon cycle during the Last Glacial–Interglacial cycle: possible role for a deepening of the mean remineralization depth and an increase in the oceanic nutrient inventory, Quaternary Science Reviews, 56, 46-68, 10.1016/j.quascirev.2012.09.012, 2012.

Mikolajewicz, U.: Modeling Mediterranean Ocean climate of the Last Glacial Maximum, Climate of the Past, 7, 161-180, 10.5194/cp-7-161-2011, 2011.

Mix, A. C., Lund, D. C., Pisias, N. G., Bodén, P., Bornmalm, L., Lyle, M. and Pike, J. : Rapid Climate Oscillations in the Northeast Pacific During the Last Deglaciation Reflect Northern and Southern Hemisphere Sources, in Mechanisms of Global Climate Change at Millennial Time Geophys. Monogr. Ser., vol. 112, edited by P. U. Clark, R. S. Webb, and L. D. Keigwin, 127–148, AGU, Washington, D. C., doi: 10.1029/GM112p0127, 1999.

Mulitza, S and A. Paul, A GUI-based synthesis toolbox for the collection, homogenization and visualization of foraminiferal stable isotope data. PMIP Ocean Workshop 2013 : Understanding Changes since the Last Glacial Maximum. Corvallis, Oregon, USA, Dec 4-6, 2013.

1449 Murakami, S., Ohgaito, R., Abe-Ouchi, A., Crucifix, M., and Otto-Bliesner, B. L.:
1450 Global-Scale Energy and Freshwater Balance in Glacial Climate: A Comparison of
1451 Three PMIP2 LGM Simulations, *Journal of Climate*, 21, 5008-5033,
1452 10.1175/2008jcli2104.1, 2008.

1453

1454 Musgrove, M., J. L. Banner, L. E. Mack, D. M. Combs, E. W. James, H. Cheng, and
1455 R. L. Edwards, Geochronology of late Pleistocene to Holocene speleothems from
1456 central Texas: Implications for regional paleoclimate, *Geol. Soc. Am. Bull.*, 113,
1457 1532–1543, doi: 10.1130/0016-7606(2001)113<1532:GOLPTH>2.0.CO;2, 2001.

1458

1459 Nikolova, I., Yin, Q., Berger, A., Singh, U. K., and Karami, M. P.: The last interglacial
1460 (Eemian) climate simulated by LOVECLIM and CCSM3, *Climate of the Past*, 9, 1789-
1461 1806, 10.5194/cp-9-1789-2013, 2013.

1462

1463 Oppo, D. W., Schmidt, G. A., and LeGrande, A. N.: Seawater isotope constraints on
1464 tropical hydrology during the Holocene, *Geophys. Res. Lett.*, 34, L13701,
1465 doi:10.1029/2007gl030017, 2007.

1466

1467 Otto-Bliesner, B. L., Rosenbloom, N., Stone, E. J., McKay, N. P., Lunt, D. J., Brady,
1468 E. C., and Overpeck, J. T.: How warm was the last interglacial? New model-data
1469 comparisons, *Philos. T. R. Soc. A*, 371, 20130097, doi:10.1098/rsta.2013.0097,
1470 2013.

1471

1472 Parrenin, F., Masson-Delmotte, V., Kohler, P., Raynaud, D., Paillard, D., Schwander,
1473 J., Barbante, C., Landais, A., Wegner, A., and Jouzel, J.: Synchronous Change of
1474 Atmospheric CO₂ and Antarctic Temperature During the Last Deglacial Warming,
1475 *Science*, 339, 1060-1063, 10.1126/science.1226368, 2013.

1476

1477 Plastino, W., and Bella, F.: Radon groundwater monitoring at underground
1478 laboratories of Gran Sasso (Italy), *Geophysical Research Letters*, 28, 2675-2677,
1479 10.1029/2000gl012430, 2001.

1480

Pol, K., Masson-Delmotte, V., Cattani, O., Debret, M., Falourd, S., Jouzel, J., Landais, A., Minster, B., Mudelsee, M., Schulz, M., and Stenni, B.: Climate variability features of the last interglacial in the East Antarctic EPICA Dome C ice core, *Geophysical Research Letters*, 41, 4004-4012, 10.1002/2014gl059561, 2014.

Rach, O., Brauer, A., Wilkes, H., and Sachse, D.: Delayed hydrological response to Greenland cooling at the onset of the Younger Dryas in western Europe, *Nature Geoscience*, 7, 109-112, 10.1038/ngeo2053, 2014.

Rasmussen, S. O., Andersen, K. K., Svensson, A. M., Steffensen, J. P., Vinther, B. M., Clausen, H. B., Siggaard-Andersen, M. L., Johnsen, S. J., Larsen, L. B., Dahl-Jensen, D., Bigler, M., Röthlisberger, R., Fischer, H., Goto-Azuma, K., Hansson, M. E., and Ruth, U.: A new Greenland ice core chronology for the last glacial termination, *J. Geophys. Res.*, 111, D06102, doi:10.1029/2005jd006079, 2006.

Reimer, P.: IntCal13 and Marine13 Radiocarbon Age Calibration Curves 0–50,000 Years cal BP, *Radiocarbon*, 55, 1869-1887, 10.2458/azu_js_rc.55.16947, 2013.

Richter, S. L., Johnson, A. H., Dranoff, M. M., LePage, B. A., and Williams, C. J.: Oxygen isotope ratios in fossil wood cellulose: Isotopic composition of Eocene- to Holocene-aged cellulose, *Geochimica et Cosmochimica Acta*, 72, 2744-2753, 10.1016/j.gca.2008.01.031, 2008.

Risi, C., Bony, S., Vimeux, F., and Jouzel, J.: Water-stable isotopes in the LMDZ4 general circulation model: model evaluation for present-day and past climates and applications to climatic interpretations of tropical isotopic records, *J. Geophys. Res.*, 115, D12118, doi:10.1029/2009jd013255, 2010.

Roche, D. M., and Caley, T.: $\delta^{18}\text{O}$ water isotope in the LOVECLIM model (version 1.0) – Part 2: Evaluation of model results against observed $\delta^{18}\text{O}$ in water samples, *Geoscientific Model Development*, 6, 1493-1504, 10.5194/gmd-6-1493-2013, 2013.

1513 Rohling, E. J., Grant, K., Hemleben, C., Siddall, M., Hoogakker, B. A. A., Bolshaw,
1514 M., and Kucera, M.: High rates of sea-level rise during the last interglacial period,
1515 Nature Geoscience, 1, 38-42, 10.1038/ngeo.2007.28, 2007.

1516
1517 Rohling, E. J., Rohling, E. J., Sluijs, A., Dijkstra, H. A., Köhler, P., van de Wal, R. S.
1518 W., von der Heydt, A. S., Beerling, D. J., Berger, A., Bijl, P. K., Crucifix, M., DeConto,
1519 R., Drijfhout, S. S., Fedorov, A., Foster, G. L., Ganopolski, A., Hansen, J., Hönlisch,
1520 B., Hooghiemstra, H., Huber, M., Huybers, P., Knutti, R., Lea, D. W., Lourens, L. J.,
1521 Lunt, D., Masson-Demotte, V., Medina-Elizalde, M., Otto-Bliesner, B., Pagani, M.,
1522 Pälike, H., Renssen, H., Royer, D. L., Siddall, M., Valdes, P., Zachos, J. C., and
1523 Zeebe, R. E.: Making sense of palaeoclimate sensitivity, Nature, 491, 683-691,
1524 10.1038/nature11574, 2012.

1525
1526 Ruth, U., Barnola, J. M., Beer, J., Bigler, M., Blunier, T., Castellano, E., Fischer, H.,
1527 Fundel, F., Huybrechts, P., Kaufmann, P., Kipfstuhl, S., Lambrecht, A., Morganti, A.,
1528 Oerter, H., Parrenin, F., Rybak, O., Severi, M., Udisti, R., Wilhelms, F., and Wolff, E.:
1529 "EDML1": a chronology for the EPICA deep ice core from Dronning Maud Land,
1530 Antarctica, over the last 150 000 years, Climate of the Past, 3, 475-484, 10.5194/cp-
1531 3-475-2007, 2007.

1532
1533 Sarnthein, M., Winn K., Duplessy J.-C., and Fontugne, M.: Global variations of
1534 surface ocean productivity in low and mid latitudes: influence on CO2 reservoirs of
1535 the deep ocean and atmosphere during the last 21,000 years, Paleoceanography,
1536 3(3), 361-399, 10.1029/PA003i003p00361, 1988.

1537
1538 Sarnthein, M., Winn, K., Jung, S. J. A., Duplessy, J.-C., Labeyrie, L., Erlenkeuser, H.,
1539 and Ganssen, G.: Changes in East Atlantic Deepwater Circulation over the last
1540 30,000 years: Eight time slice reconstructions, Paleoceanography, 9, 209-267,
1541 10.1029/93pa03301, 1994.

1542
1543 Schaefer, J. M.: Near-Synchronous Interhemispheric Termination of the Last Glacial
1544 Maximum in Mid-Latitudes, Science, 312, 1510-1513, 10.1126/science.1122872,
1545 2006.

1546

1547 Schmidt, G. A., Annan, J. D., Bartlein, P. J., Cook, B. I., Guilyardi, E., Hargreaves, J.
 1548 C., Harrison, S. P., Kageyama, M., LeGrande, A. N., Konecky, B., Lovejoy, S., Mann,
 1549 M. E., Masson-Delmotte, V., Risi, C., Thompson, D., Timmermann, A., Tremblay, L.
 1550 B., and Yiou, P.: Using palaeo-climate comparisons to constrain future projections in
 1551 CMIP5, *Climate of the Past*, 10, 221-250, 10.5194/cp-10-221-2014, 2014.
 1552
 1553 Schmidt, G. A., LeGrande, A. N., and Hoffmann, G.: Water isotope expressions of
 1554 intrinsic and forced variability in a coupled ocean–atmosphere model, *J. Geophys.*
 1555 *Res.*, 112, D10103, doi:10.1029/2006jd007781, 2007.
 1556
 1557 Shakun, J. D., Clark, P. U., He, F., Marcott, S. A., Mix, A. C., Liu, Z., Otto-Bliesner,
 1558 B., Schmittner, A., and Bard, E.: Global warming preceded by increasing carbon
 1559 dioxide concentrations during the last deglaciation, *Nature*, 484, 49-54,
 1560 10.1038/nature10915, 2012.
 1561
 1562 Shin, S.-I.: Southern Ocean sea-ice control of the glacial North Atlantic thermohaline
 1563 circulation, *Geophys. Res. Lett.*, 30(2), 1096, doi:10.1029/2002gl015513, 2003.
 1564
 1565 Siani, G., Michel, E., De Pol-Holz, R., DeVries, T., Lamy, F., Carel, M., Isguder, G.,
 1566 Dewilde, F., and Laurantou, A.: Carbon isotope records reveal precise timing of
 1567 enhanced Southern Ocean upwelling during the last deglaciation, *Nat. Commun.*, 4,
 1568 2758, doi:10.1038/ncomms3758, 2013.
 1569
 1570 Sikes, E. L., and T. P. Guilderson (2016), Southwest Pacific Ocean surface reservoir
 1571 ages since the last glaciation: Circulation insights from multiple-core studies,
 1572 *Paleoceanography*, 31, 298–310, doi:10.1002/2015PA002855.
 1573
 1574 Sime, L. C., Risi, C., Tindall, J. C., Sjolte, J., Wolff, E. W., Masson-Delmotte, V., and
 1575 Capron, E.: Warm climate isotopic simulations: what do we learn about interglacial
 1576 signals in Greenland ice cores?, *Quaternary Science Reviews*, 67, 59-80,
 1577 10.1016/j.quascirev.2013.01.009, 2013.
 1578

1579 Sime, L. C., Wolff, E. W., Oliver, K. I. C., and Tindall, J. C.: Evidence for warmer
1580 interglacials in East Antarctic ice cores, *Nature*, 462, 342-345, 10.1038/nature08564,
1581 2009.

1583 Skinner, L. C., Fallon, S., Waelbroeck, C., Michel, E., and Barker, S.: Ventilation of
1584 the Deep Southern Ocean and Deglacial CO₂ Rise, *Science*, 328, 1147-1151,
1585 10.1126/science.1183627, 2010.

1587 Smith, J. A., Mark, B. G., and Rodbell, D. T.: The timing and magnitude of mountain
1588 glaciation in the tropical Andes, *Journal of Quaternary Science*, 23, 609-634,
1589 10.1002/jqs.1224, 2008.

1591 Sortor, R. N., and Lund, D. C.: No evidence for a deglacial intermediate water $\Delta^{14}\text{C}$
1592 anomaly in the SW Atlantic, *Earth and Planetary Science Letters*, 310, 65-72,
1593 10.1016/j.epsl.2011.07.017, 2011.

1595 Soulet, G., Ménot, G., Garreta, V., Rostek, F., Zaragosi, S., Lericolais, G., and Bard,
1596 E.: Black Sea “Lake” reservoir age evolution since the Last Glacial — Hydrologic and
1597 climatic implications, *Earth and Planetary Science Letters*, 308, 245-258,
1598 10.1016/j.epsl.2011.06.002, 2011.

1600 Sperling, M., Schmiedl, G., Hemleben, C., Emeis, K. C., Erlenkeuser, H., and
1601 Grootes, P. M.: Black Sea impact on the formation of eastern Mediterranean sapropel
1602 S1? Evidence from the Marmara Sea, *Palaeogeography, Palaeoclimatology,*
1603 *Palaeoecology*, 190, 9-21, 10.1016/s0031-0182(02)00596-5, 2003.

1605 Sprowl, D.R.: On the precision of the Elk Lake varve chronology. In Bradbury, J.P. ,
1606 editor, *Elk Lake, Minnesota: evidence for rapid climate change in the north-central*
1607 *United States*. Boulder CO: Geological Society of America : Special Paper 276, 69-
1608 74, 1993.

1610 Steig, E. J., and Orsi, A. J.: Climate Science: The heat is on in Antarctica, *Nature*
1611 *Geoscience*, 6, 87-88, 10.1038/ngeo1717, 2013.

Steig, E. J., Schneider, D. P., Rutherford, S. D., Mann, M. E., Comiso, J. C., and Shindell, D. T.: Warming of the Antarctic ice-sheet surface since the 1957 International Geophysical Year, *Nature*, 457, 459-462, 10.1038/nature07669, 2009.

Sternberg, L. d. S. L. O. R.: Oxygen stable isotope ratios of tree-ring cellulose: the next phase of understanding, *New Phytologist*, 181, 553-562, 10.1111/j.1469-8137.2008.02661.x, 2009.

Stocker, T. F.: The Seesaw Effect, *Sci.* , 282 (5386), 61–62, doi:10.1126/science.282.5386.61 , 1998.

Stott, L., Timmermann, A., and Thunell, R.: Southern Hemisphere and Deep-Sea Warming Led Deglacial Atmospheric CO₂ Rise and Tropical Warming, *Science*, 318, 435-438, 10.1126/science.1143791, 2007.

Stott, L.: Super ENSO and Global Climate Oscillations at Millennial Time Scales, *Science*, 297, 222-226, 10.1126/science.1071627, 2002.

Stuiver, M., & Braziunas, T. F.: Tree cellulose ¹³C/¹²C isotope ratios and climatic change. *Nature*, 328(6125), 58–60. doi:10.1038/328058a0, 1987.

Sturm, C., Zhang, Q., and Noone, D.: An introduction to stable water isotopes in climate models: benefits of forward proxy modelling for paleoclimatology, *Climate of the Past*, 6, 115-129, 10.5194/cp-6-115-2010, 2010.

Sun, Y., Oppo, D. W., Xiang, R., Liu, W., and Gao, S.: Last deglaciation in the Okinawa Trough: subtropical northwest Pacific link to Northern Hemisphere and tropical climate, *Paleoceanography*, 20, PA4005 doi:10.1029/2004pa001061, 2005.

Switsur, R., Waterhouse, J.: Stable isotopes in tree ring cellulose. In: Griffiths, H. (Ed.), *Stable Isotopes: Integration of Biological, Ecological and Geochemical Processes*. BIOS Scientific Publishers Ltd., Oxford, pp. 303–321, 1998.

1646 Sylvestre, F.: Moisture pattern during the last glacial maximum in South America in
 1647 Past climate variability from the Last Glacial Maximum to the Holocene in South
 1648 America and Surrounding regions, in: Developments in Paleoenvironmental
 1649 Research Series (DPER), edited by: Vimeux, F., Sylvestre, F., and Khodri, M.,
 1650 Springer, New York, Vol. 14, XVII, 418 p. 106 illus., 61 in color., ISBN 978-90-481-
 1651 2671-2, 2009.

1652

1653 Tagliabue, A., Bopp, L., Roche, D. M., Bouttes, N., Dutay, J. C., Alkama, R.,
 1654 Kageyama, M., Michel, E., and Paillard, D.: Quantifying the roles of ocean circulation
 1655 and biogeochemistry in governing ocean carbon-13 and atmospheric carbon dioxide
 1656 at the last glacial maximum, *Climate of the Past*, 5, 695-706, 10.5194/cp-5-695-2009,
 1657 2009.

1658

1659 Tessin, A. C., and Lund, D. C.: Isotopically depleted carbon in the mid-depth South
 1660 Atlantic during the last deglaciation, *Paleoceanography*, 28, 296-306,
 1661 10.1002/palo.20026, 2013.

1662

1663 Tindall, J. C., Valdes, P. J., and Sime, L. C.: Stable water isotopes in HadCM3:
 1664 isotopic signature of El Niño–Southern Oscillation and the tropical amount effect, *J.*
 1665 *Geophys. Res.*, 114, D04111, doi:10.1029/2008jd010825, 2009.

1666

1667 Tudhope, A. W.: Variability in the El Niño-Southern Oscillation Through a Glacial-
 1668 Interglacial Cycle, *Science*, 291, 1511-1517, 10.1126/science.1057969, 2001.

1669

1670 Turner, J., Colwell, S. R., Marshall, G. J., Lachlan-Cope, T. A., Carleton, A. M.,
 1671 Jones, P. D., Lagun, V., Reid, P. A., and Iagovkina, S.: Antarctic climate change
 1672 during the last 50 years, *International Journal of Climatology*, 25, 279-294,
 1673 10.1002/joc.1130, 2005.

1674

1675 Van Campo, E.: Monsoon fluctuations in two 20,000-Yr B.P. Oxygen-isotope/pollen
 1676 records off southwest India, *Quaternary Research*, 26, 376-388, 10.1016/0033-
 1677 5894(86)90097-9, 1986.

1678

1679 Veres, D., Bazin, L., Landais, A., Toyé Mahamadou Kele, H., Lemieux-Dudon, B.,
1680 Parrenin, F., Martinerie, P., Blayo, E., Blunier, T., Capron, E., Chappellaz, J.,
1681 Rasmussen, S. O., Severi, M., Svensson, A., Vinther, B., and Wolff, E. W.: The
1682 Antarctic ice core chronology (AICC2012): an optimized multi-parameter and multi-
1683 site dating approach for the last 120 thousand years, *Clim. Past*, 9, 1733-1748,
1684 doi:10.5194/cp-9-1733-2013, 2013.

1685
1686 Vimeux F., de Angelis M., Ginot P., Magand O., Pouyaud B., Casassa G., Johnsen
1687 S., Falourd S., A promising location in Patagonia for paleoclimate and environmental
1688 reconstructions revealed by a shallow firn core from Monte San Valentin (Northern
1689 Patagonia Icefield, Chile), *Journal of Geophysical Research*, 113, D16118,
1690 doi:10.1029/2007JD009502, 2008.

1691
1692 Vimeux F., Gallaire R., Bony S., Hoffmann G., Chiang. J. and Fuertes R. , What are
1693 the climate controls on isotopic composition (dD) of precipitation in Zongo Valley
1694 (Bolivia) ? Implications for the Illimani ice core interpretation, *Earth and Planetary
1695 Sciences Letters*, 240, 205-220, 2005.

1696
1697 Vimeux F., Ginot P., Schwikowski M., Vuille M., Hoffmann G., Thompson L.G.,
1698 Schotterer U, Climate variability during the last 1000 years inferred from Andean ice
1699 cores: a review of methodology and recent results, *Palaeogeography,
1700 Palaeoclimatology, Palaeoecology*, 281, 229-241, doi:10.1016/j.palaeo.2008.03.054,
1701 2009a.

1702
1703 Vimeux, F.: Similarities and discrepancies between Polar and Andean ice cores over
1704 the last deglaciation in Past climate variability from the Last Glacial Maximum to the
1705 Holocene in South America and Surrounding regions, in: Developments in
1706 Paleoenvironmental Research Series (DPER), edited by: Vimeux, F., Sylvestre, F.,
1707 and Khodri, M., Springer, New York, Vol. 14, XVII, 418 p. 106 illus., 61 in color., ISBN
1708 978-90-481-2671-2, 2009b.

1709
1710 Vinther, B. M., Buchardt, S. L., Clausen, H. B., Dahl-Jensen, D., Johnsen, S. J.,
1711 Fisher, D. A., Koerner, R. M., Raynaud, D., Lipenkov, V., Andersen, K. K., Blunier, T.,

1712 Rasmussen, S. O., Steffensen, J. P., and Svensson, A. M.: Holocene thinning of the
 1713 Greenland ice sheet, *Nature*, 461, 385-388, 10.1038/nature08355, 2009.
 1714
 1715 Vinther, B. M., Clausen, H. B., Johnsen, S. J., Rasmussen, S. O., Andersen, K. K.,
 1716 Buchardt, S. L., Dahl-Jensen, D., Seierstad, I. K., Siggaard-Andersen, M. L.,
 1717 Steffensen, J. P., Svensson, A., Olsen, J., and Heinemeier, J.: A synchronized dating
 1718 of three Greenland ice cores throughout the Holocene, *J. Geophys. Res.*, 111,
 1719 D13102, doi:10.1029/2005jd006921, 2006.
 1720
 1721 Waelbroeck, C., Duplessy, J.-C., Michel, E., Labeyrie, L., Paillard, D., and Duprat, J.:
 1722 The timing of the last deglaciation in North Atlantic climate records, *Nature*, 412,
 1723 724–727, doi:10.1038/35089060, 2001.
 1724
 1725 Waelbroeck, C., Paul, A., Kucera, M., Rosell-Melé, A., Weinelt, M., Schneider, R.,
 1726 Mix, A. C., Abellmann, A., Armand, L., Bard, E., Barker, S., Barrows, T. T., Benway,
 1727 H., Cacho, I., Chen, M. T., Cortijo, E., Crosta, X., de Vernal, A., Dokken, T., Duprat,
 1728 J., Elderfield, H., Eynaud, F., Gersonde, R., Hayes, A., Henry, M., Hillaire-Marcel, C.,
 1729 Huang, C. C., Jansen, E., Juggins, S., Kallel, N., Kiefer, T., Kienast, M., Labeyrie, L.,
 1730 Leclaire, H., Londeix, L., Mangin, S., Matthiessen, J., Marret, F., Meland, M., Morey,
 1731 A. E., Mulitza, S., Pflaumann, U., Pisias, N. G., Radi, T., Rochon, A., Rohling, E. J.,
 1732 Sbaifi, L., Schäfer-Neth, C., Solignac, S., Spero, H., Tachikawa, K., and Turon, J. L.:
 1733 Constraints on the magnitude and patterns of ocean cooling at the Last Glacial
 1734 Maximum, *Nature Geoscience*, 2, 127-132, 10.1038/ngeo411, 2009.
 1735
 1736 Wainer, K., Genty, D., Blamart, D., Daëron, M., Bar-Matthews, M., Vonhof, H.,
 1737 Dublyansky, Y., Pons-Branchu, E., Thomas, L., van Calsteren, P., Quinif, Y., and
 1738 Caillon, N.: Speleothem record of the last 180 ka in Villars cave (SW France):
 1739 Investigation of a large $\delta^{18}\text{O}$ shift between MIS6 and MIS5, *Quaternary Science*
 1740 *Reviews*, 30, 130-146, 10.1016/j.quascirev.2010.07.004, 2011.
 1741
 1742 Wang, Y. J., Cheng, H., Edwards, R. L., He, Y. Q., Kong, X. G., An, Z. S., Wu, J. Y.,
 1743 Kelly, M. J., Dykoski, C. A., and Li, X. D.: The Holocene Asian monsoon: Links to

1744 solar changes and North Atlantic climate, *Science*, 308(5723), 854–857,
1745 doi:10.1126/science.1106296, 2005.

1746
1747 Wang, Y. J., Cheng, H., Edwards, R. L., An, Z. S., Wu, J. Y., Shen, C. C., & Dorale,
1748 J. a.: A high-resolution absolute-dated late Pleistocene Monsoon record from Hulu
1749 Cave, China. *Science* (New York, N.Y.), 294(5550), 2345–2348.
1750 doi:10.1126/science.1064618, 2001.

1751
1752 Weldeab, S., Schneider, R. R., and Kölling, M.: Deglacial sea surface temperature
1753 and salinity increase in the western tropical Atlantic in synchrony with high latitude
1754 climate instabilities, *Earth and Planetary Science Letters*, 241, 699-706,
1755 10.1016/j.epsl.2005.11.012, 2006.

1756
1757 Werner, M., Langebroek, P. M., Carlsen, T., Herold, M., and Lohmann, G.: Stable
1758 water isotopes in the ECHAM5 general circulation model: toward high-resolution
1759 isotope modeling on a global scale, *J. Geophys. Res.*, 116, D15109,
1760 doi:10.1029/2011jd015681, 2011.

1761
1762 Yoshimura, K., Frankenberg, C., Lee, J., Kanamitsu, M., Worden, J., and Röckmann,
1763 T.: Comparison of an isotopic atmospheric general circulation model with new
1764 quasiglobal satellite measurements of water vapor isotopologues, *J. Geophys. Res.*,
1765 116, D19118, doi:10.1029/2011jd016035, 2011.

1766
1767 Yoshimura, K., Kanamitsu, M., Noone, D., and Oki, T.: Historical isotope simulation
1768 using Reanalysis atmospheric data, *J. Geophys. Res.*, 113, D19108,
1769 doi:10.1029/2008jd010074, 2008.

1770
1771 Yoshimura, K., Miyazaki, S., Kanae, S., and Oki, T.: Iso-MATSIRO, a land surface
1772 model that incorporates stable water isotopes, *Global and Planetary Change*, 51, 90-
1773 107, 10.1016/j.gloplacha.2005.12.007, 2006.

1774

1775 Yu, E.-F., Francois, R., and Bacon, M. P.: Similar rates of modern and last-glacial
1776 ocean thermohaline circulation inferred from radiochemical data, *Nature*, 379, 689-
1777 694, 10.1038/379689a0, 1996.
1778
1779 Yuan, D., H. Cheng, R.L. Edwards, C.A. Dykoski, M.J. Kelly, M. Zhang, J. Qing, Y.
1780 Lin, Y. Wang, J. Wu, J.A. Dorale, Z. An, and Y. Cai. Last Interglacial Asian
1781 Monsoon. *Science*, Vol. 304, Issue 5670, 575-578, 2004.
1782
1783 Zuraida, R., Holbourn, A., Nürnberg, D., Kuhnt, W., Dürkop, A., and Erichsen, A.:
1784 Evidence for Indonesian throughflow slowdown during Heinrich events 3–5,
1785 *Paleoceanography*, 24, PA2205, doi:10.1029/2008pa001653, 2009.
1786

Figure captions

Figure 1: Web portal screen captures illustrating the search criteria (A), the resulting maps (B), and the time series plot (C).

Figure 2: Number of publications and records in the database versus year of publication.

Figure 3: Map indicating the position of archives with different symbols representing the type of archive for dated $\delta^{18}\text{O}$ (top) $\delta^{13}\text{C}$ (center) and δD records (bottom) available on the online portal. Note that these maps only display the location of dated records, and stack and multi-sites composite records are not included.

Figure 4: Diagram showing the distribution of ice cores, tree-ring, lacustrine, speleothem and marine records as a function of latitude ($^{\circ}$).

Figure 5: Diagram showing the distribution of ice cores, tree-ring, lacustrine, speleothem and marine records as a function of coring site elevation.

Figure 6: Diagrams showing the number of $\delta^{18}\text{O}$ and $\delta^{13}\text{C}$ records from marine and lake cores, speleothems, ice cores, and tree ring cellulose for each PMIP time slice.

Figure 7: Location of lacustrine (triangles), speleothems (squares) and marine records (circles) where chronological information is available, and with quality flags for age model quality evaluation.

Figure 8: Map showing the location of $\delta^{18}\text{O}$ records spanning the MH and PD with the symbols reflecting the type of source archive and colors documenting the amplitude of $\delta^{18}\text{O}$ variations between these two periods (MH-PD). The bottom figure shows the color scale as well as the fraction of records as a function of the MH-PD $\delta^{18}\text{O}$ anomaly. Note the non-linear scale for $\delta^{18}\text{O}$ difference. The $\delta^{18}\text{O}$ difference from marine records was reversed for coherency with the sign of changes of terrestrial

1819 records. Note that some proximate core-sites may not be visible on the figure
1820 because of graphical overlaps.

1821

1822 **Figure 9:** Same as Fig. 8 but for the difference between LIG and MH values (LIG-
1823 MH).

1824

1825 **Figure 10 :** Same as Fig. 8 but between the MH and the LGM (LGM-MH).

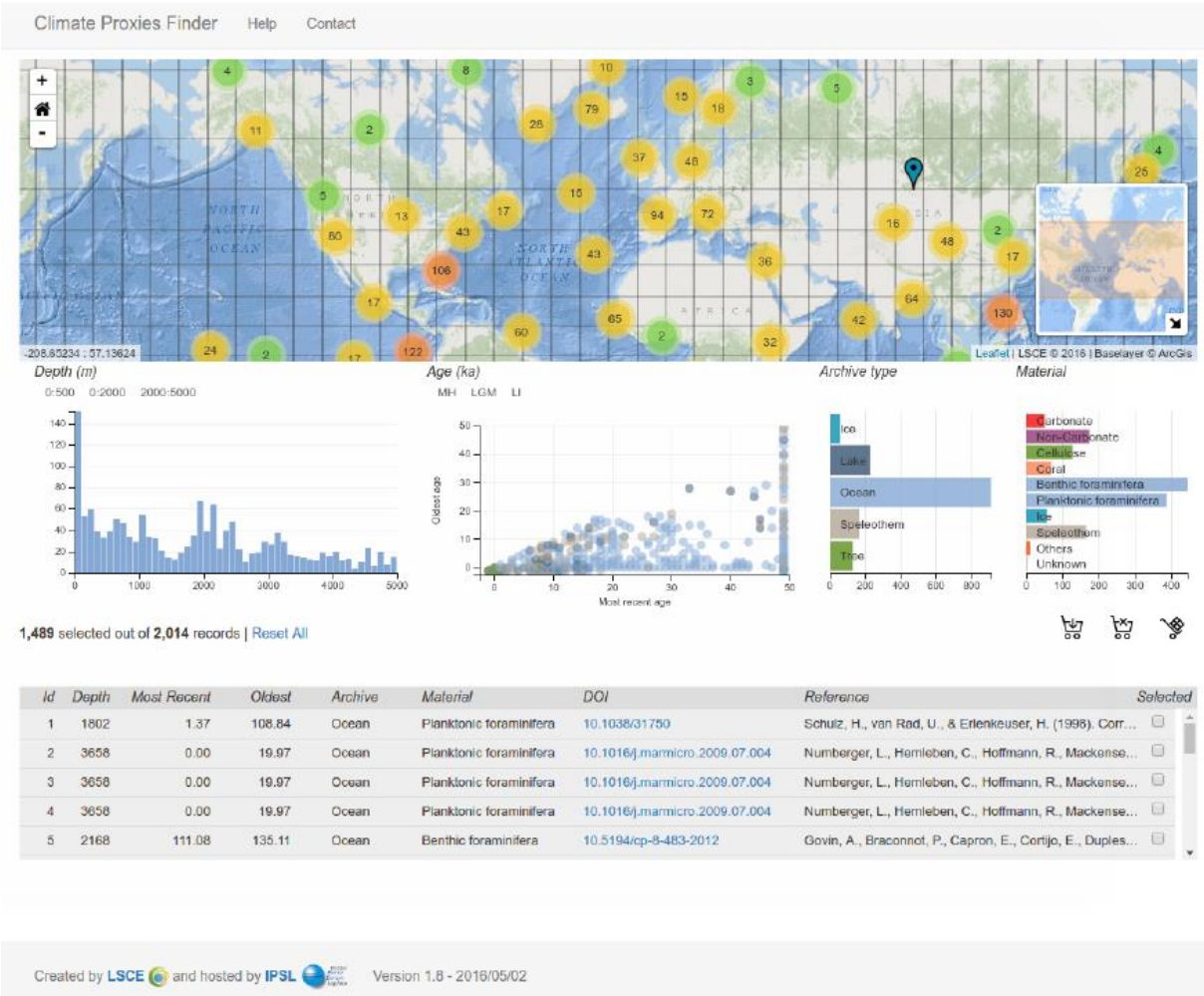
1826

1827 **Figures**

1828

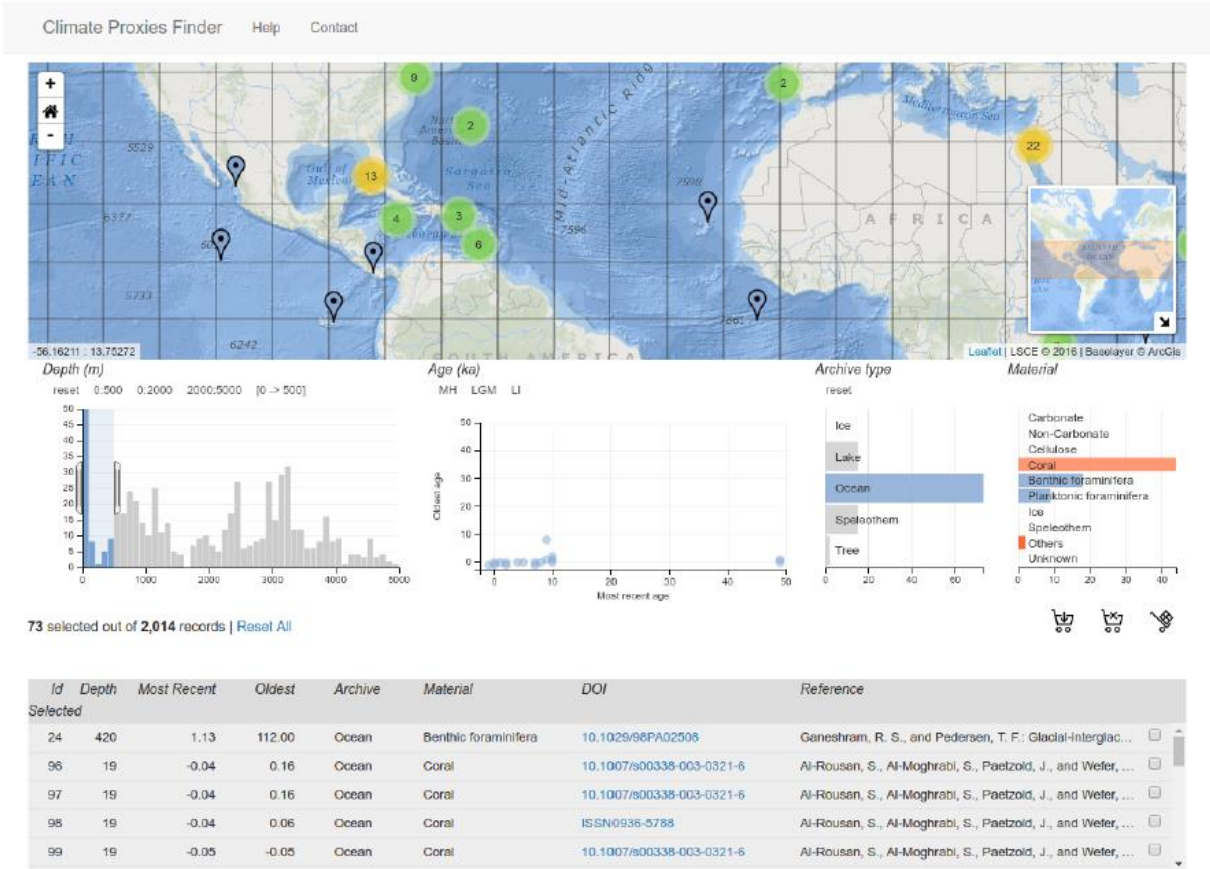
1829 **Figure 1**

A



1830

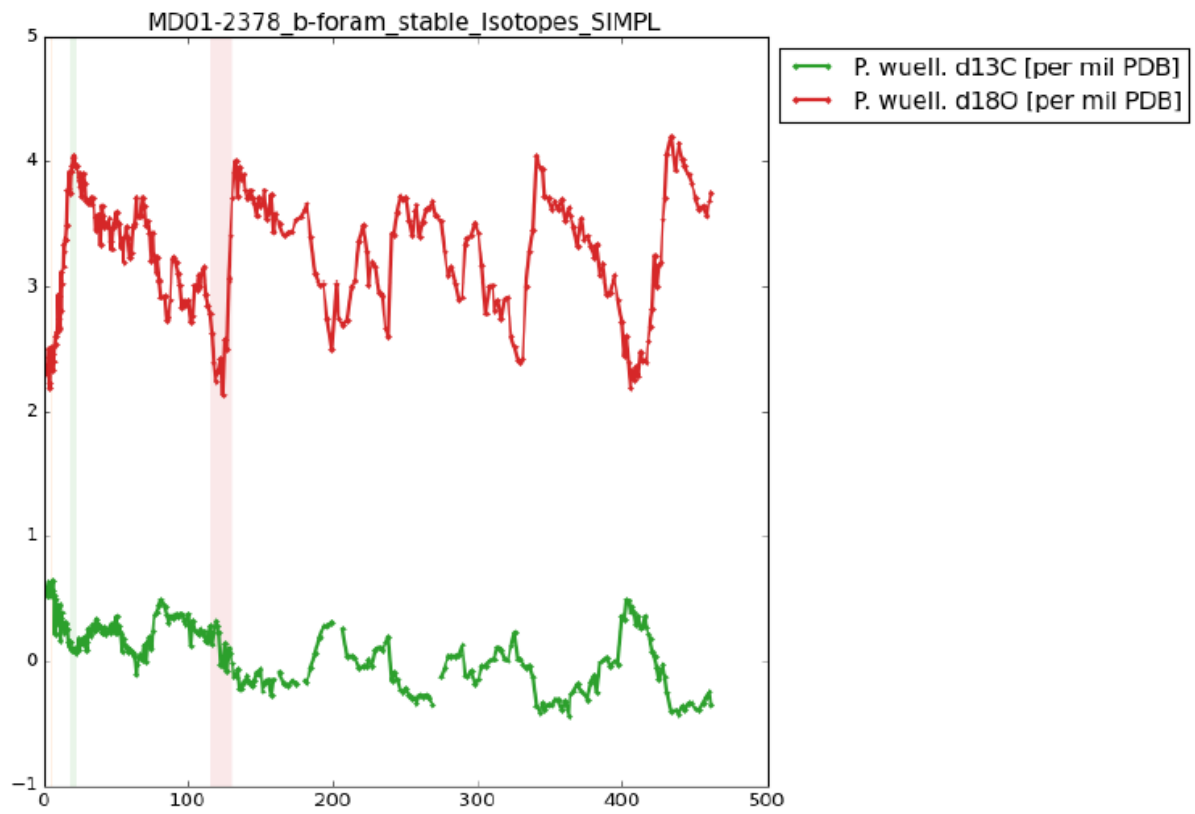
B



1831

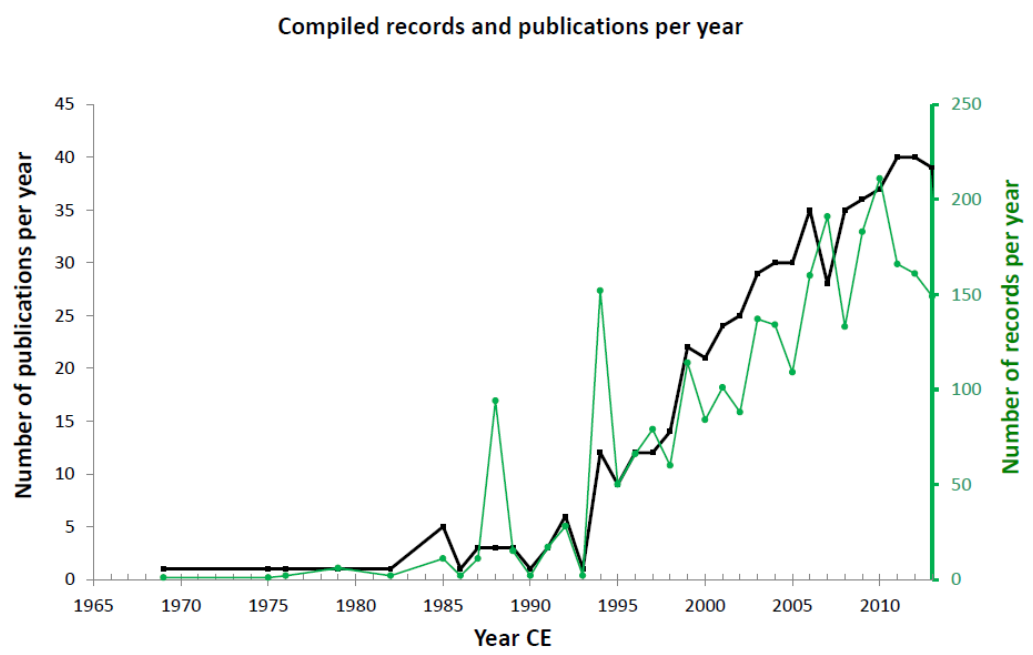
1832

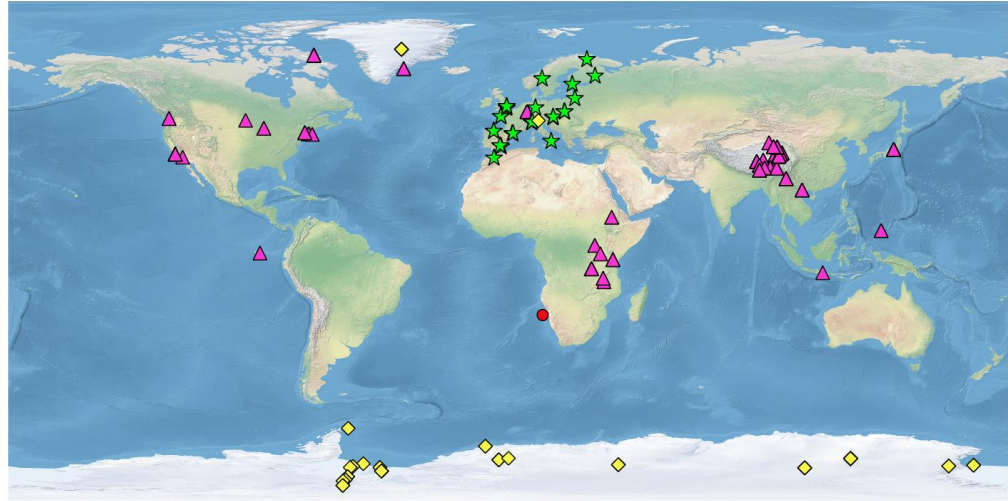
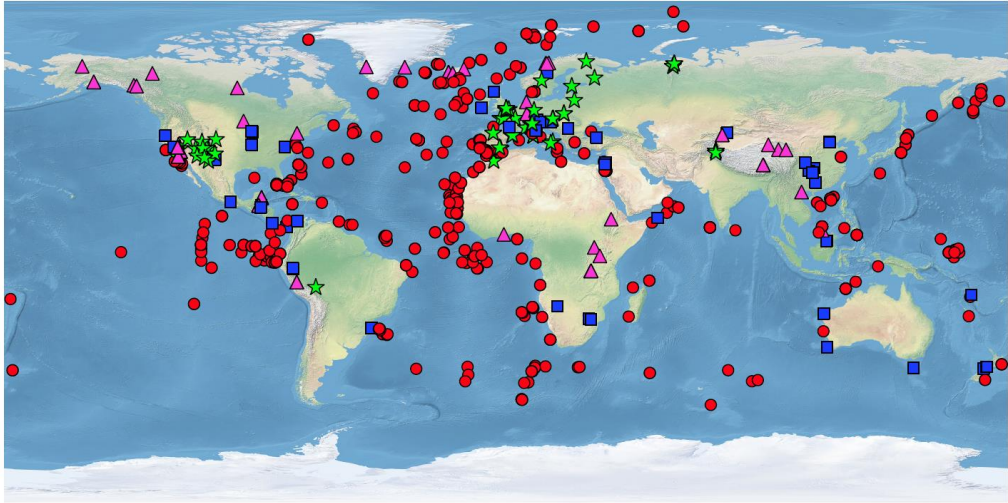
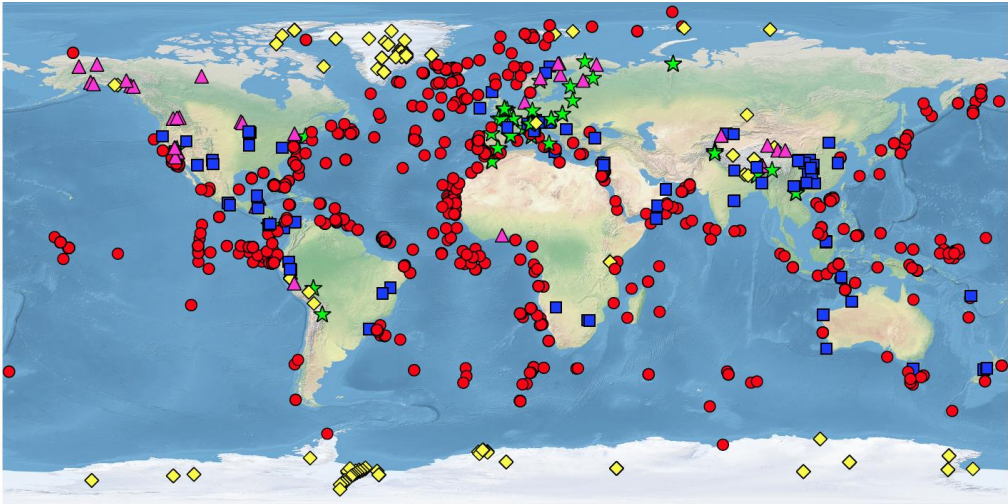
C



1833

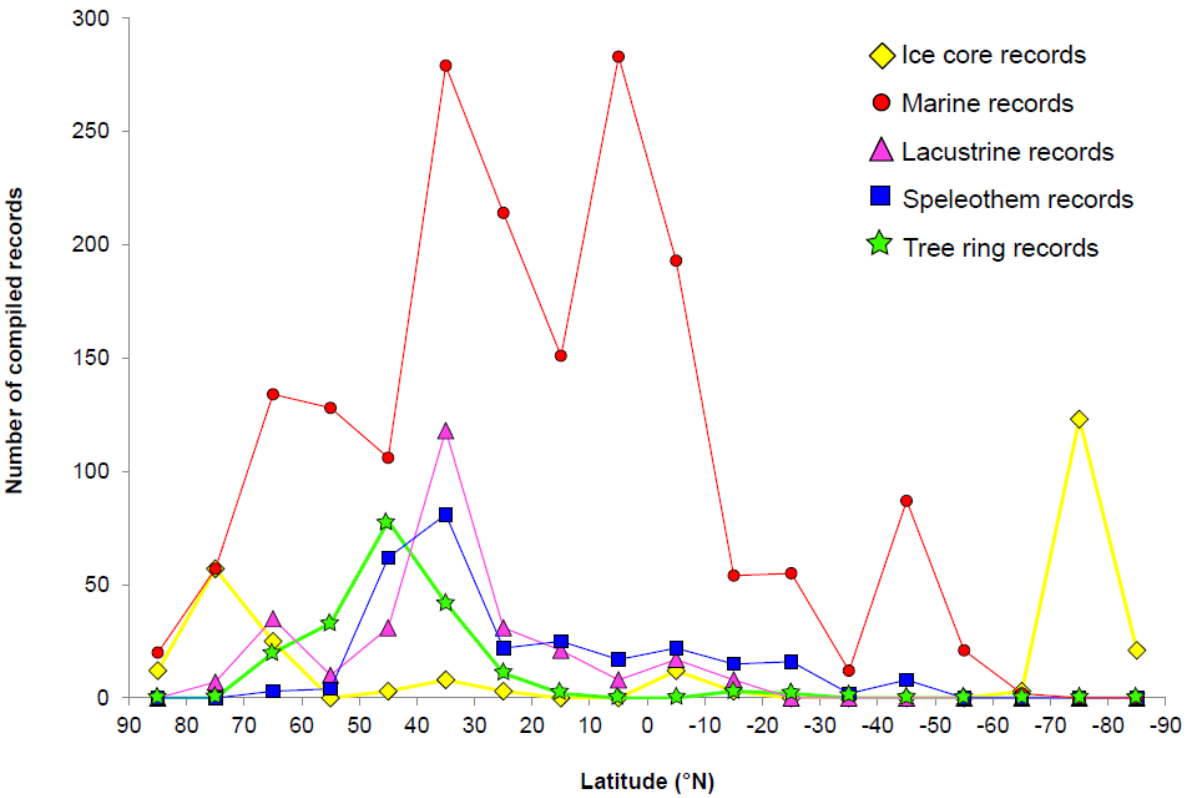
1834





● Marine cores ■ Speleothems ★ Tree rings cellulose ▲ Lacustrine cores ◆ Ice cores

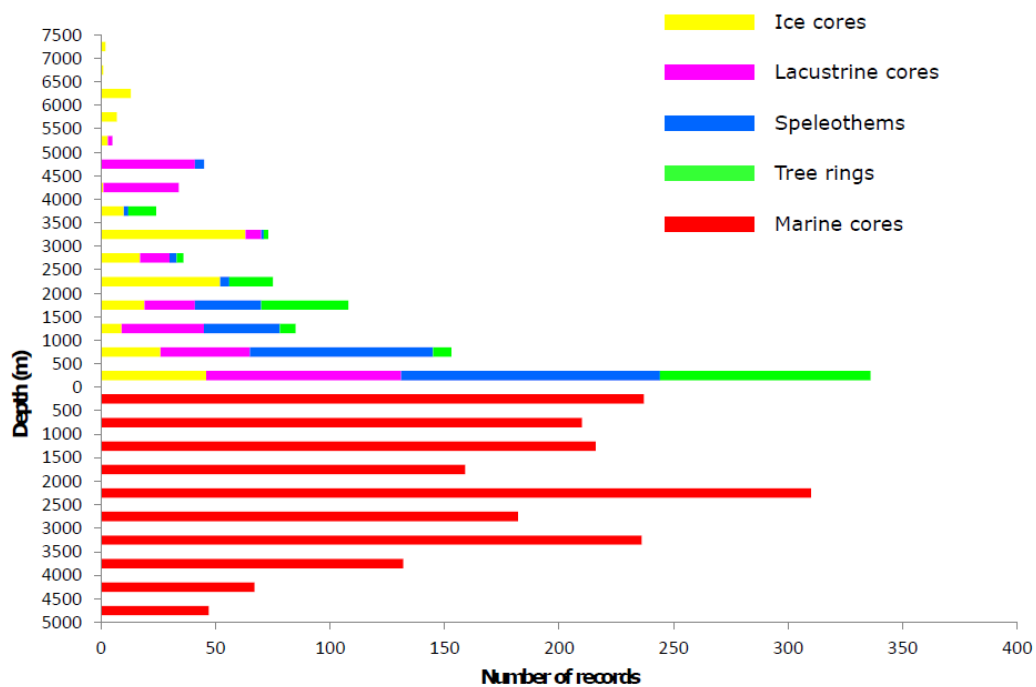
1841 **Figure 4**



1842

1843

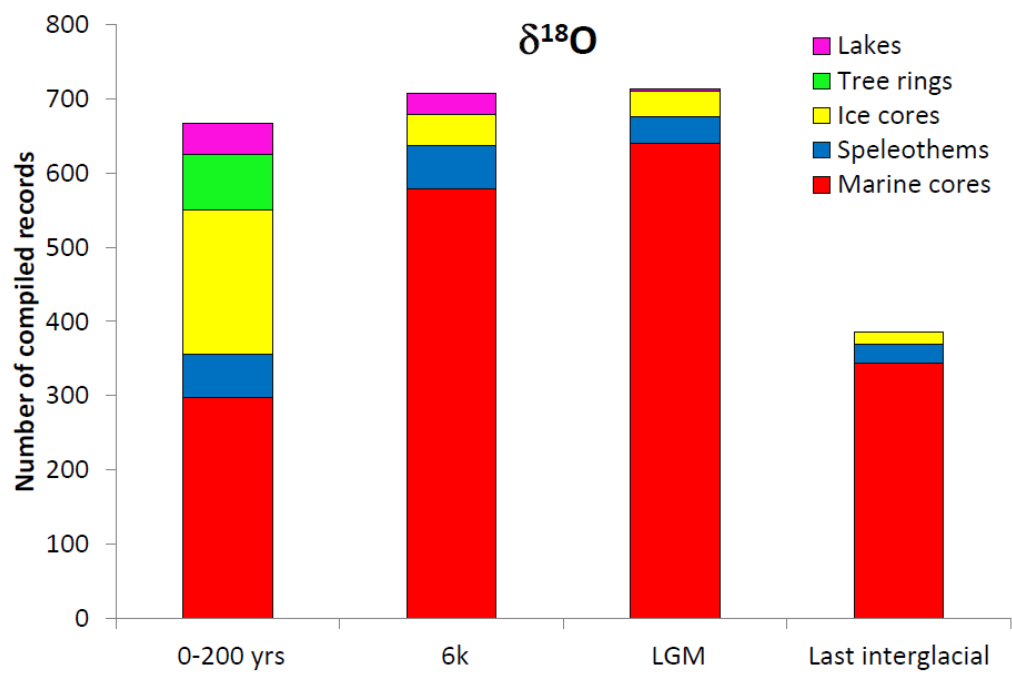
1844 **Figure 5**



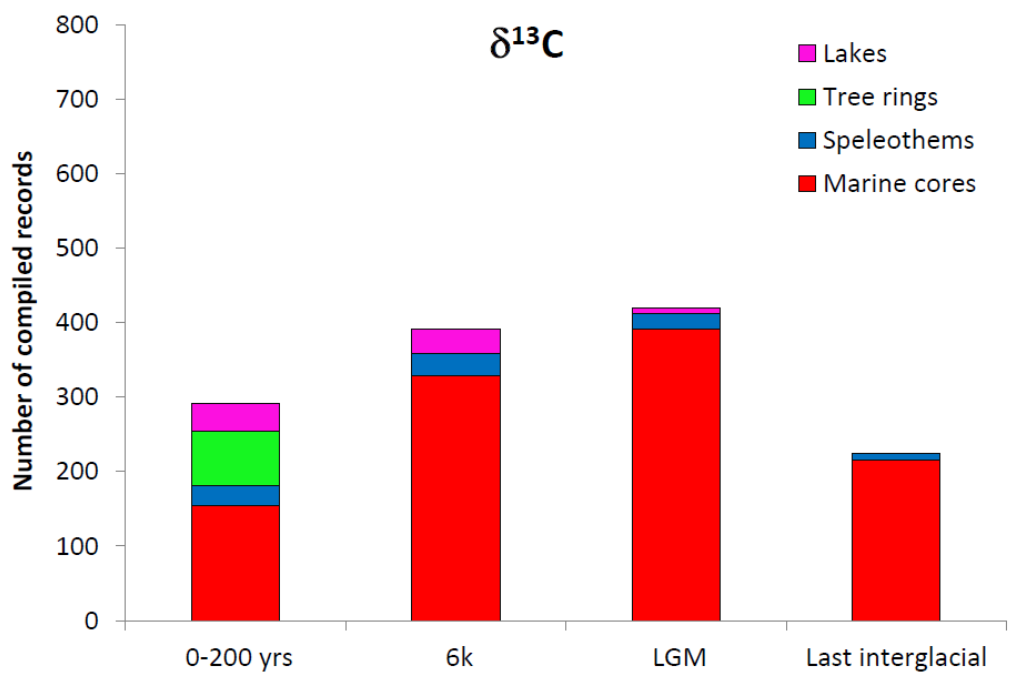
1845

1846

1847 **Figure 6**

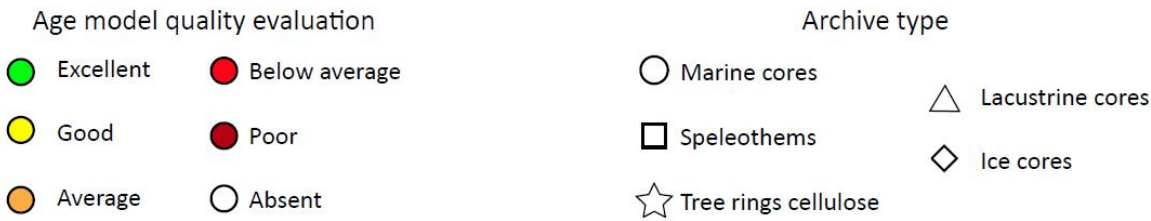
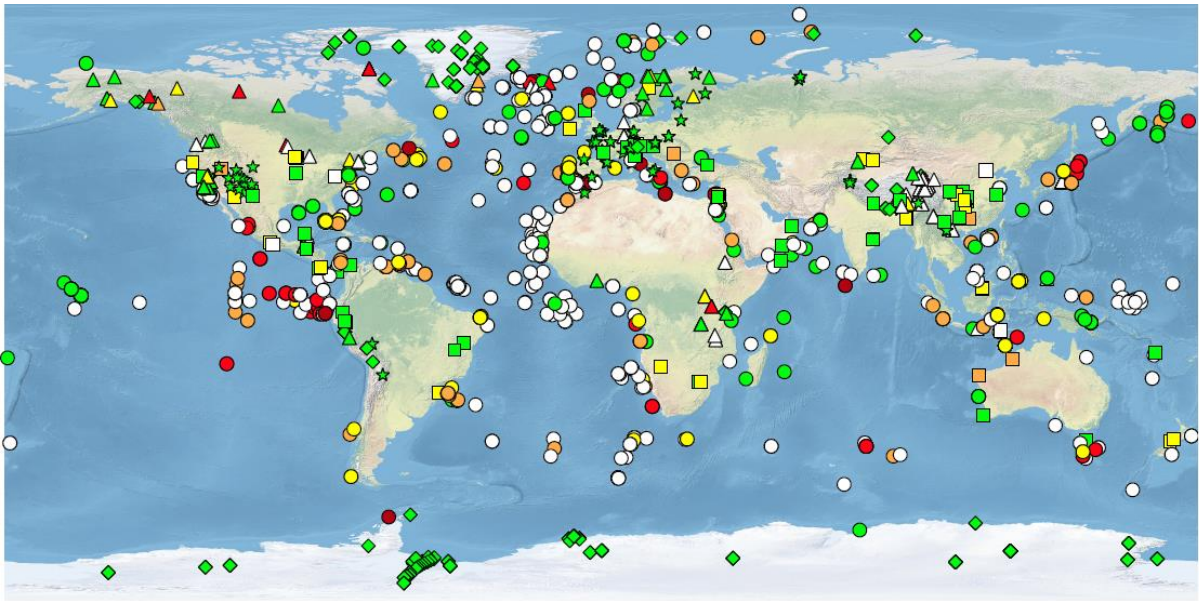


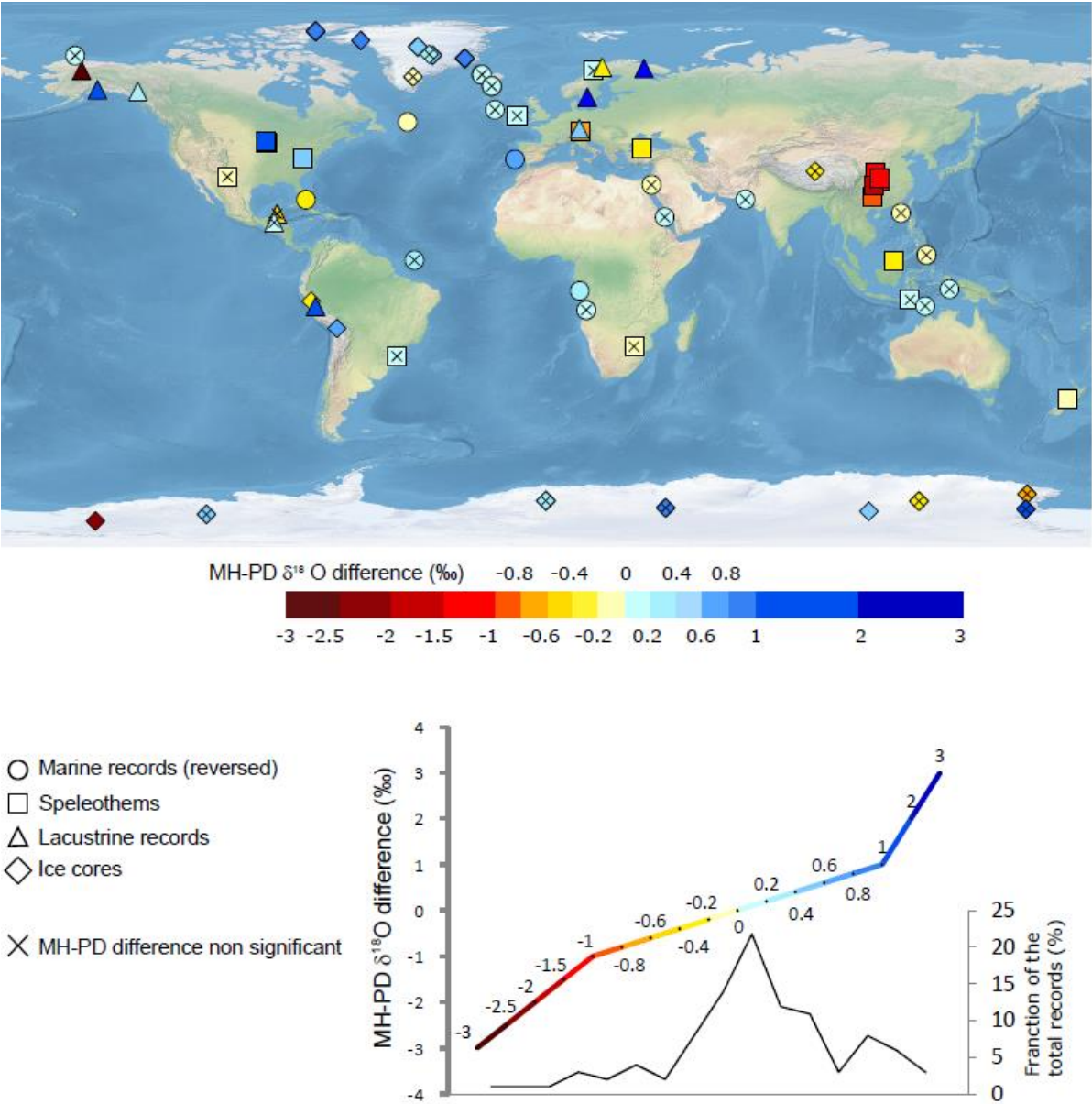
1848



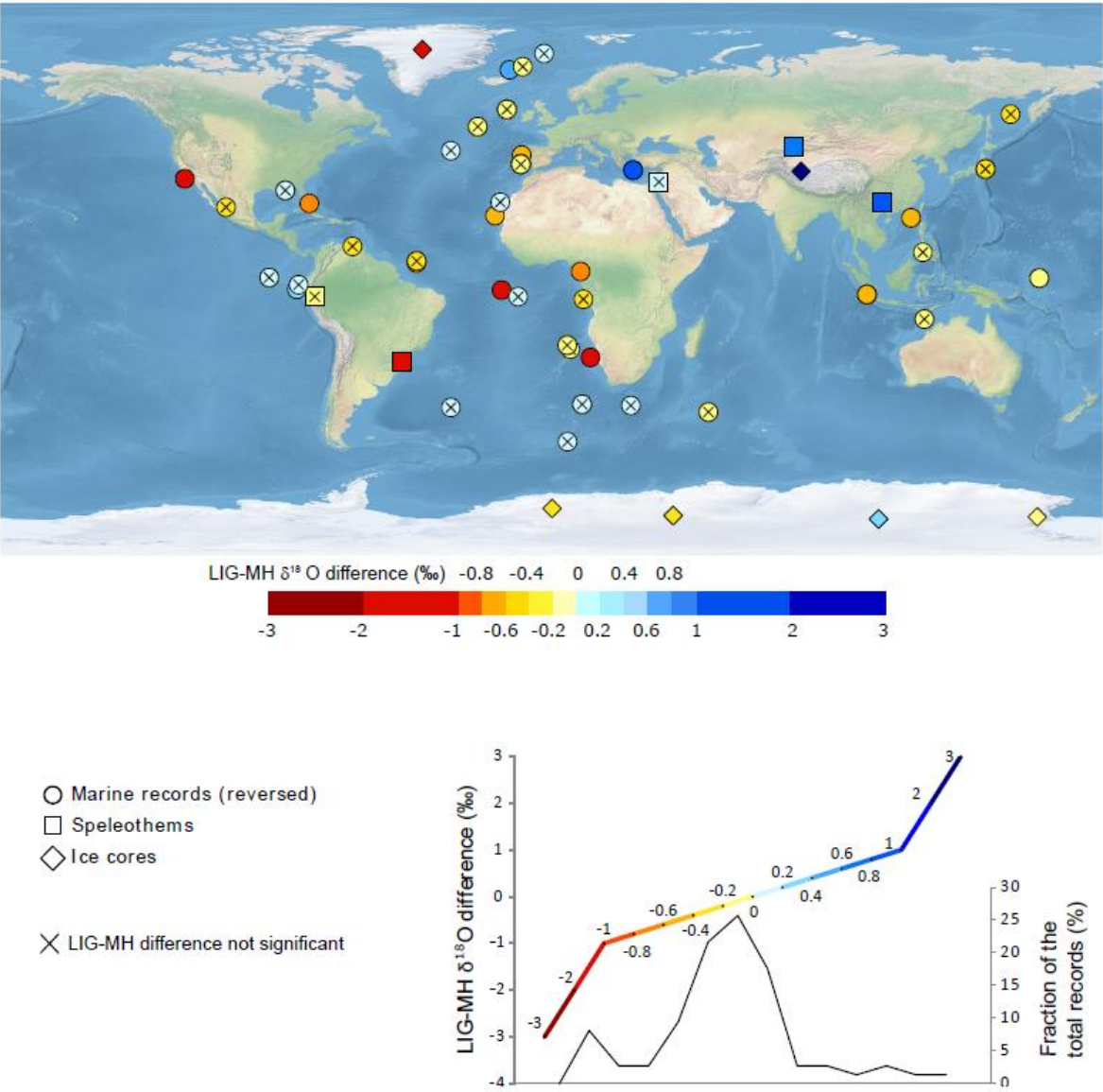
1849

1850





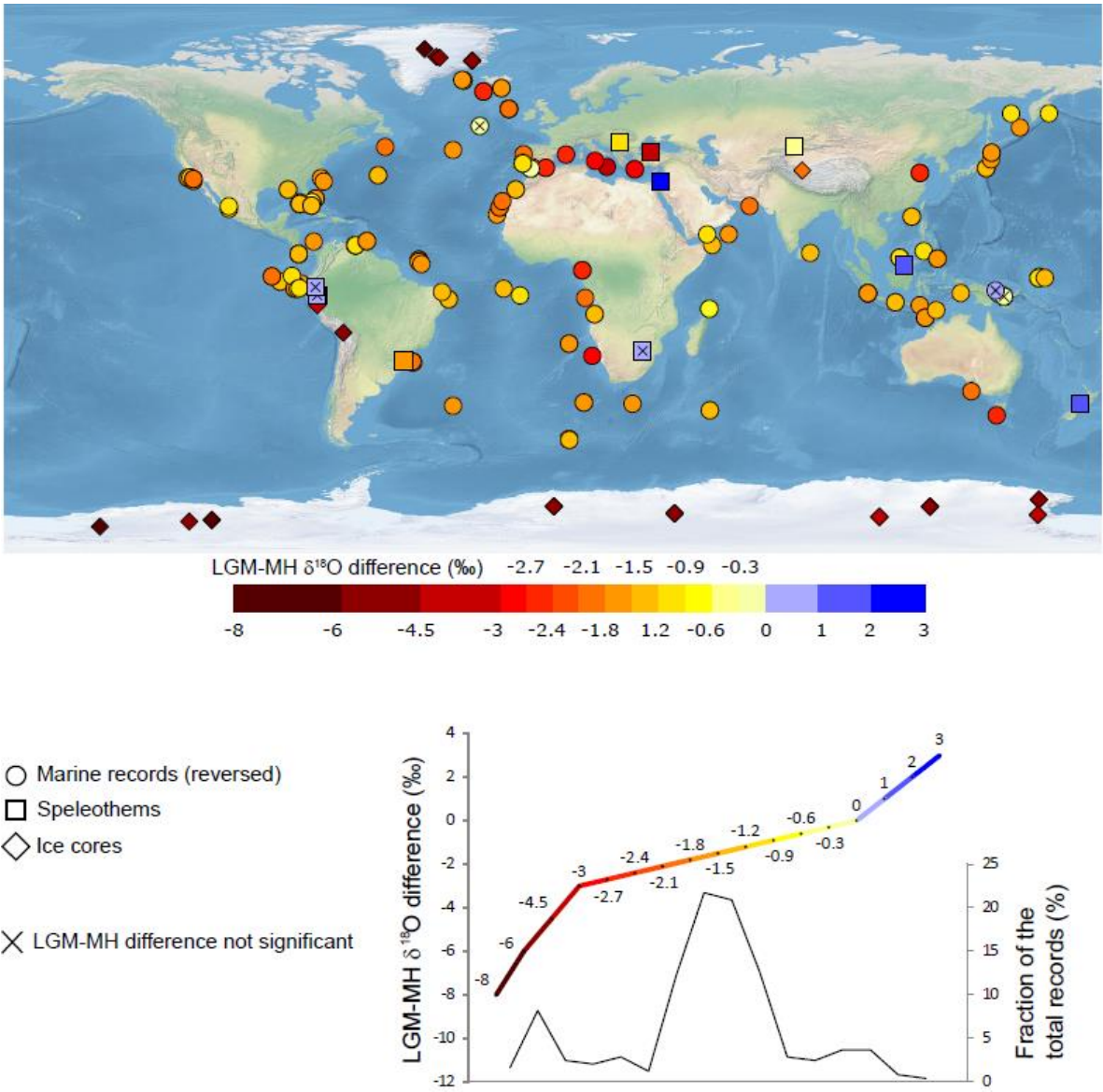
1857 **Figure 9**



1858

1859

Figure 10



Appendix

Statistical analysis – Estimation of the significance of the offset between PMIP time slices.

The significance of the difference between two different PMIP time slices (A and B) was assessed by simply comparing the offset between the average isotopic value of these two periods (\bar{A} and \bar{B}), to the average value of the standard deviations of the isotopic record for each of the two periods (σ_A and σ_B).

$$\bar{A} - \bar{B} \Leftrightarrow \frac{(\sigma_A + \sigma_B)}{2}$$

We consider that the isotopic offset is (not) significant if the absolute value of the offset is greater (smaller) than the average standard deviation along the two periods.

Figure captions

Figure A1: Diagrams showing the distribution of records (number of records) as a function of their mean time resolution (number of data points) for the different types of archives compiled in the database for the Present day (1800-2013 CE). Note the different vertical scales.

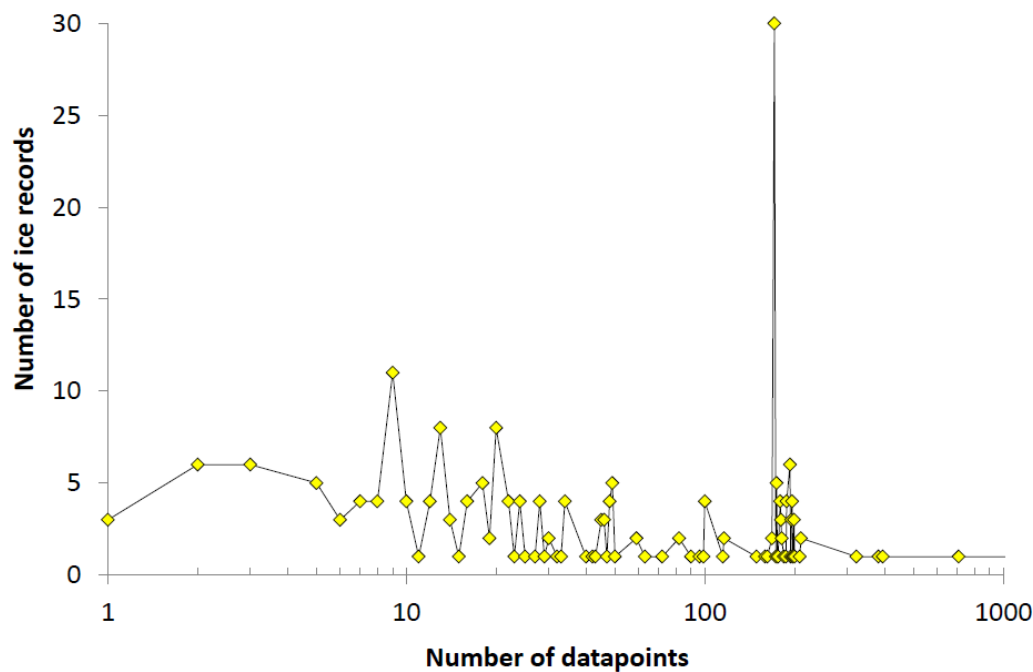
Figure A2: Same as Figure 1 but for the Mid-Holocene (5.5-6.5 ka). Note the different vertical scales.

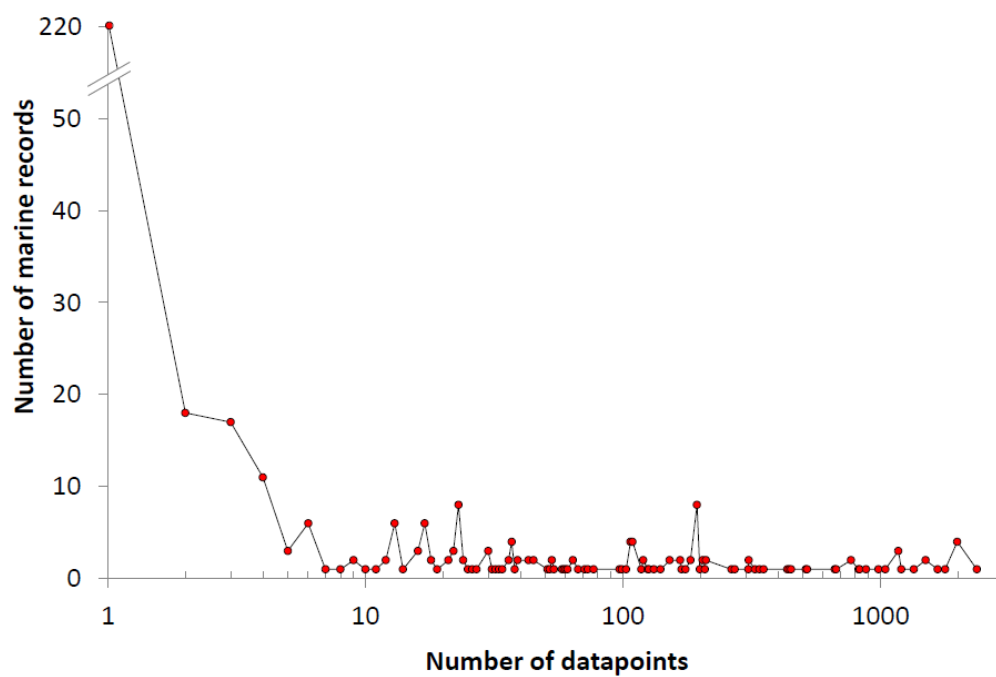
Figure A3: Same as Figure 1 but for the LGM (19-23 ka). Note the different vertical scales.

Figure A4: Same as Figure 1 but for the last Interglacial (115-130 ka). Note the different vertical scales.

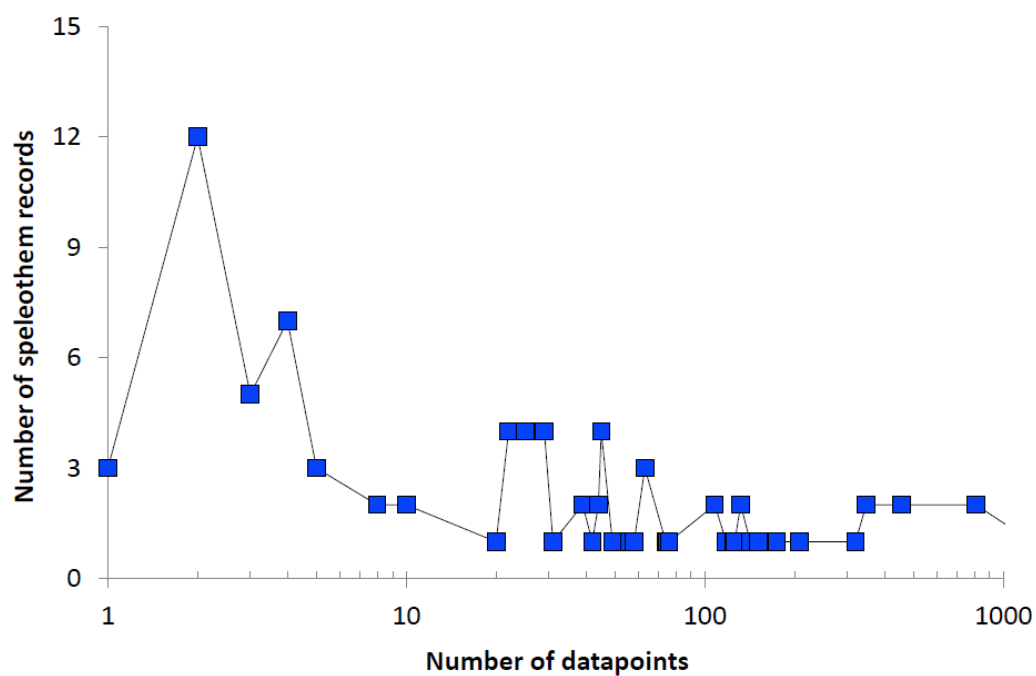
Appendix Figures

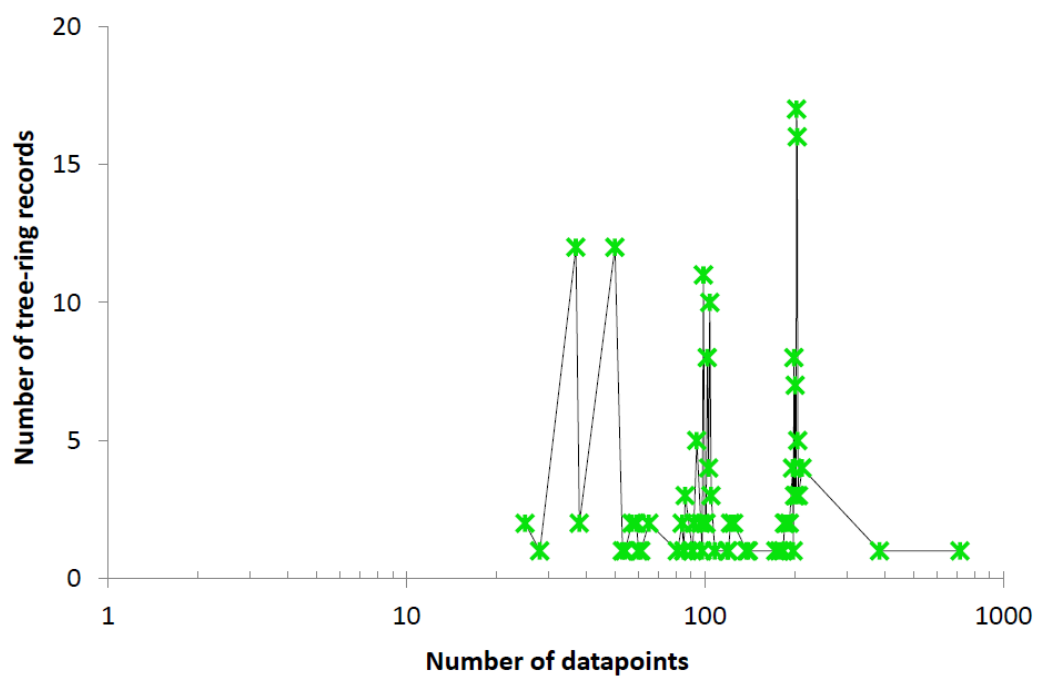
Figure A1





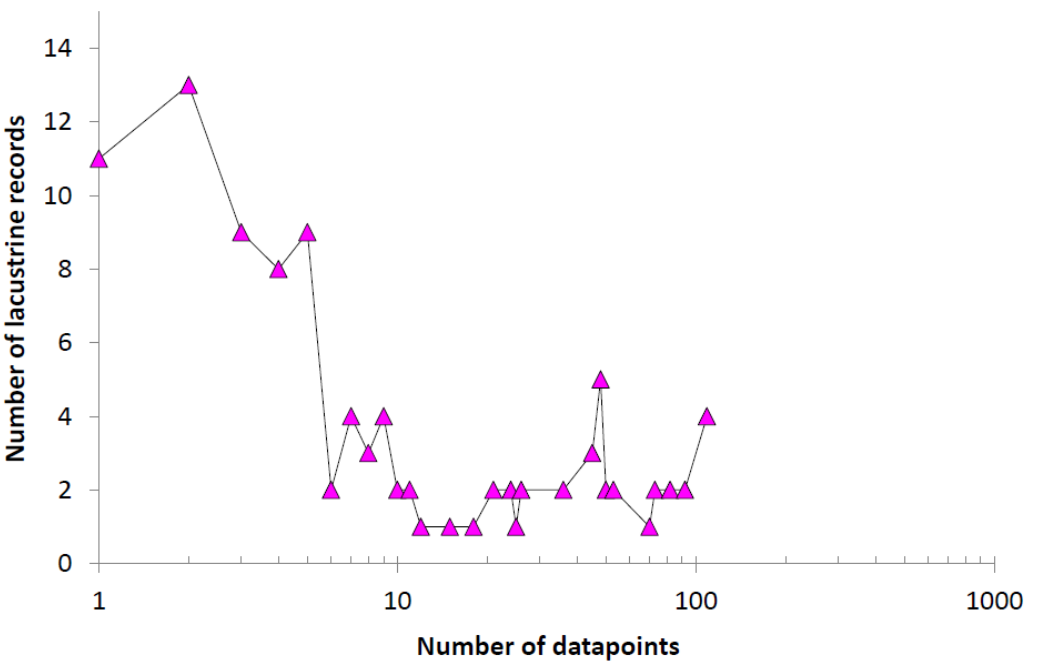
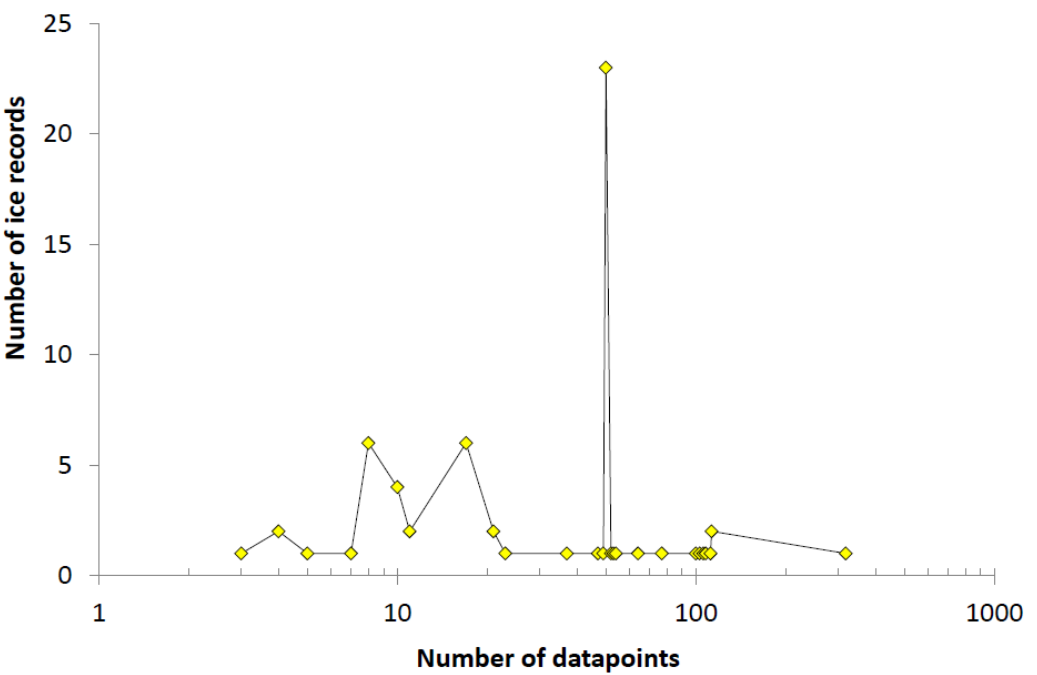
1900

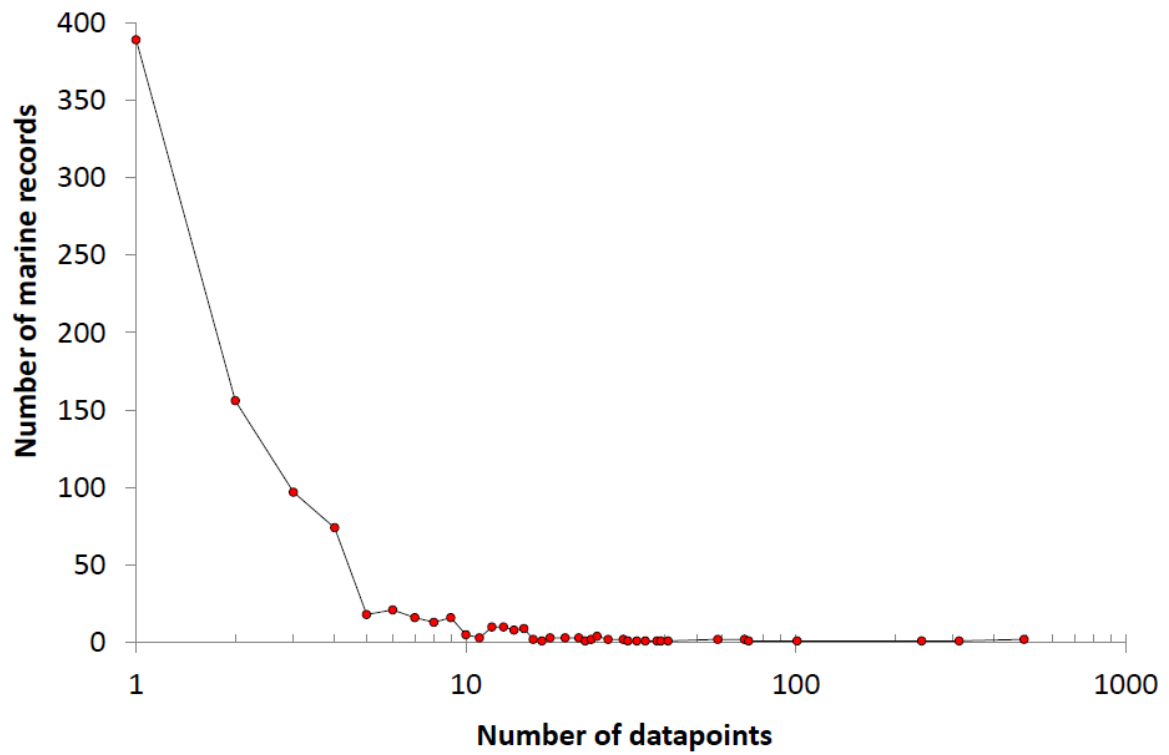




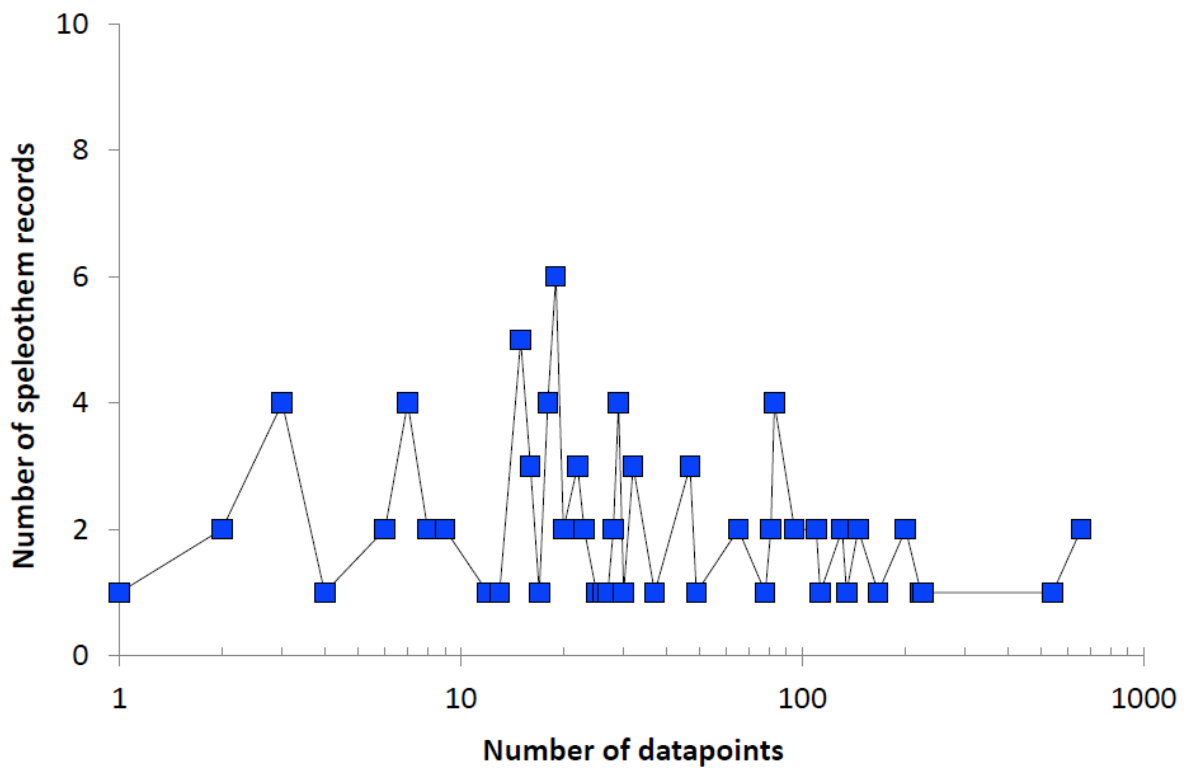
1902

1903





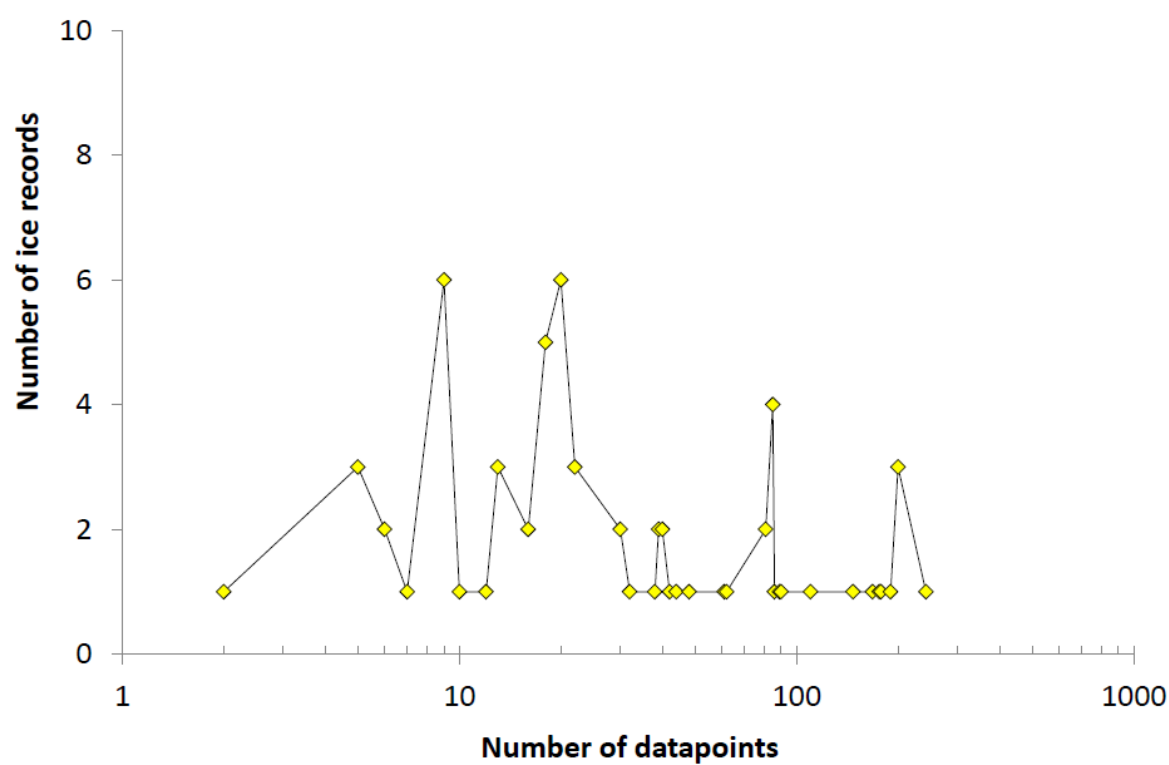
1907



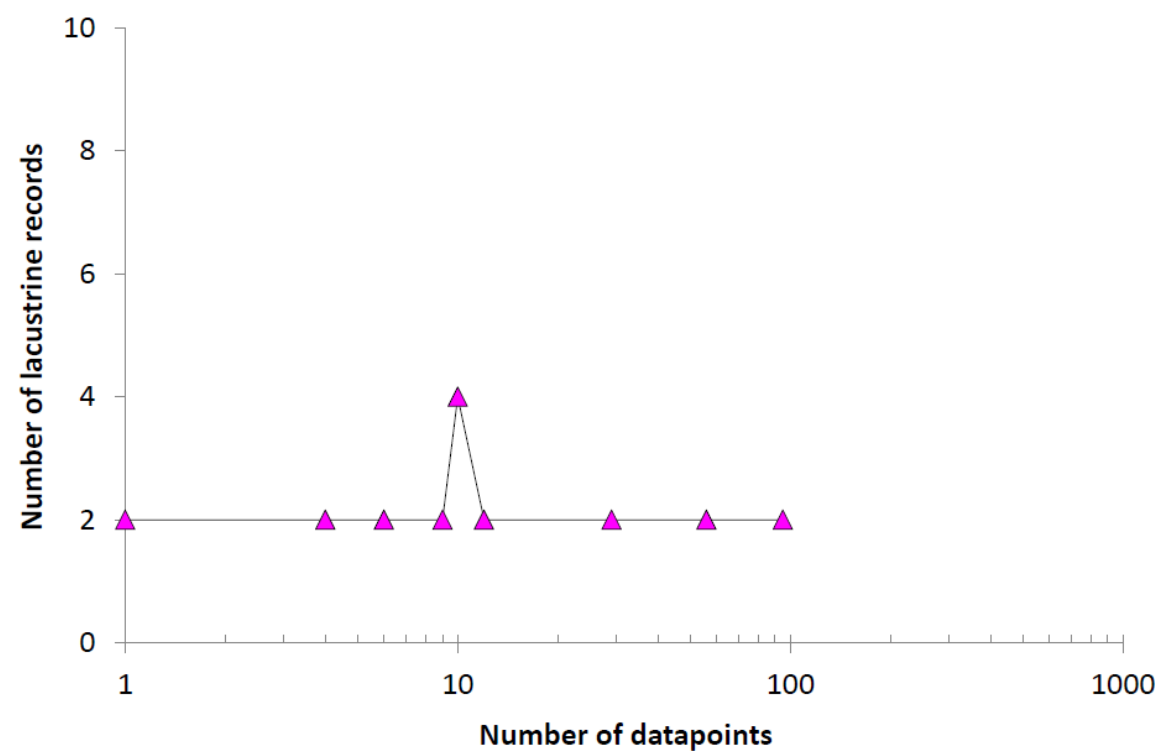
1908

1909

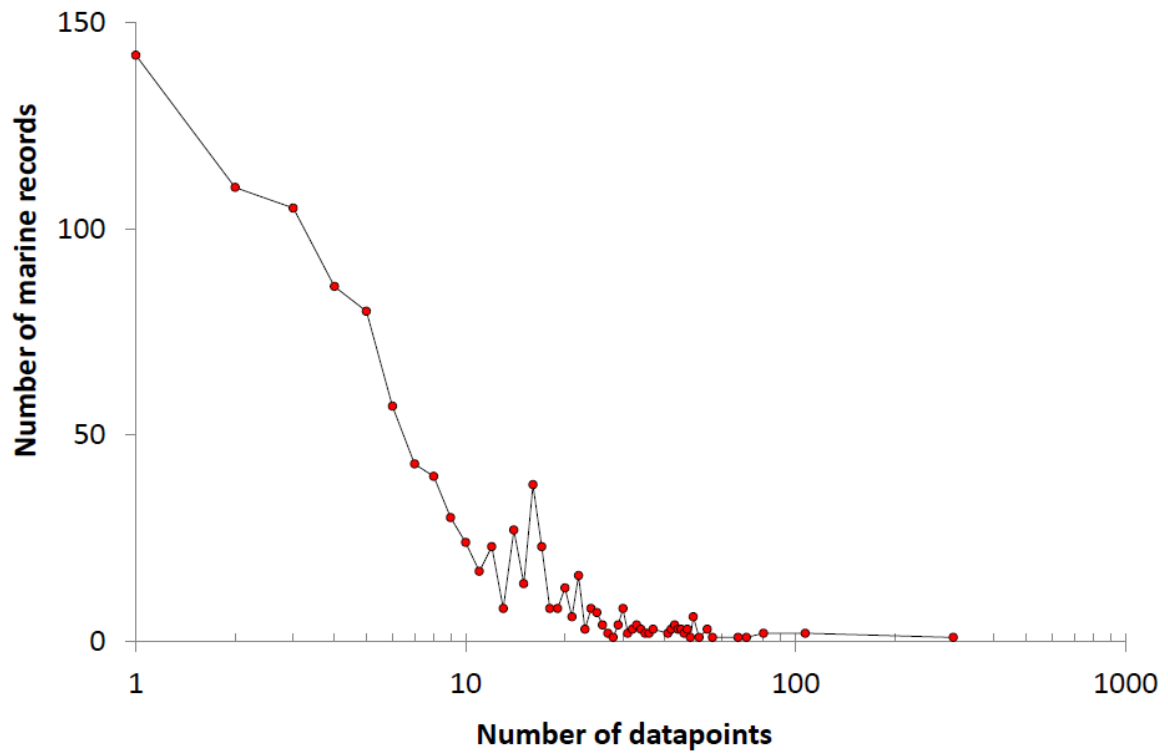
1910 **Figure A3**



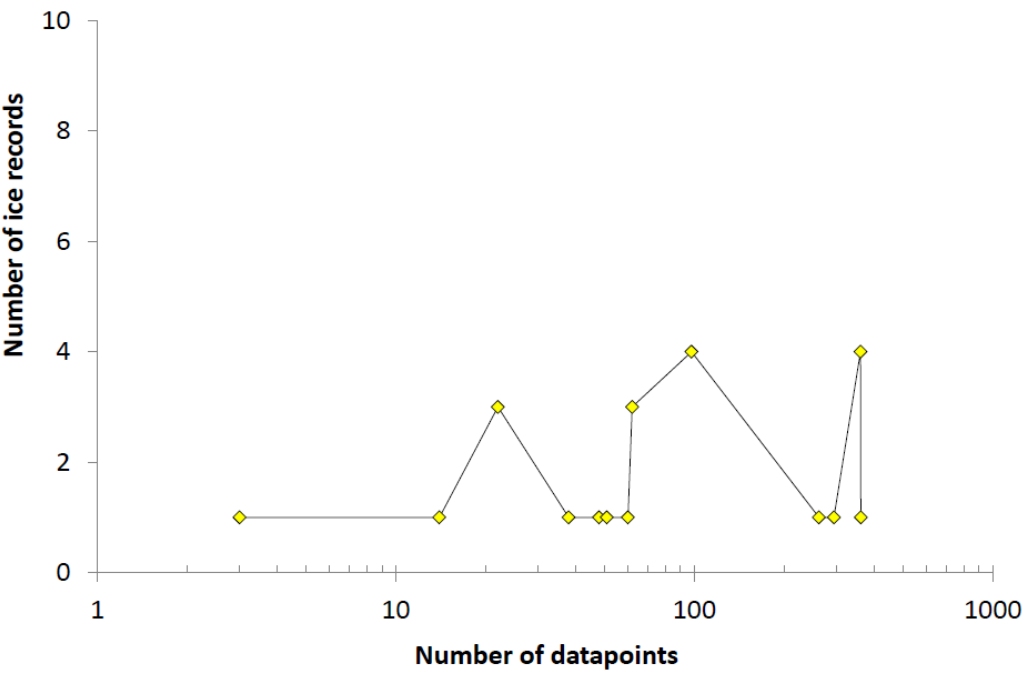
1911



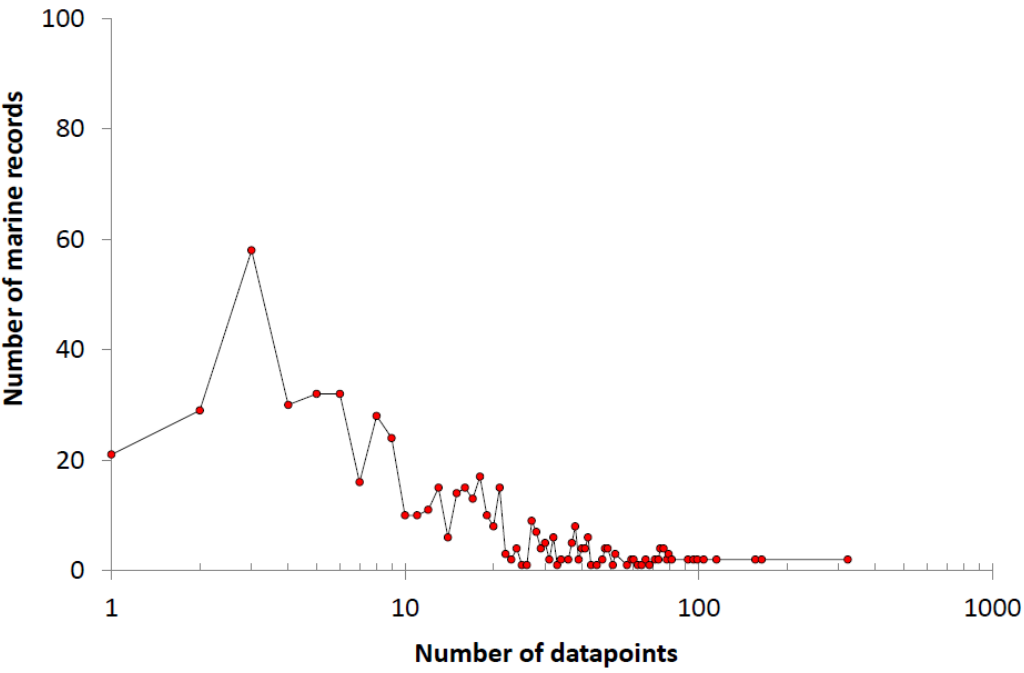
1912

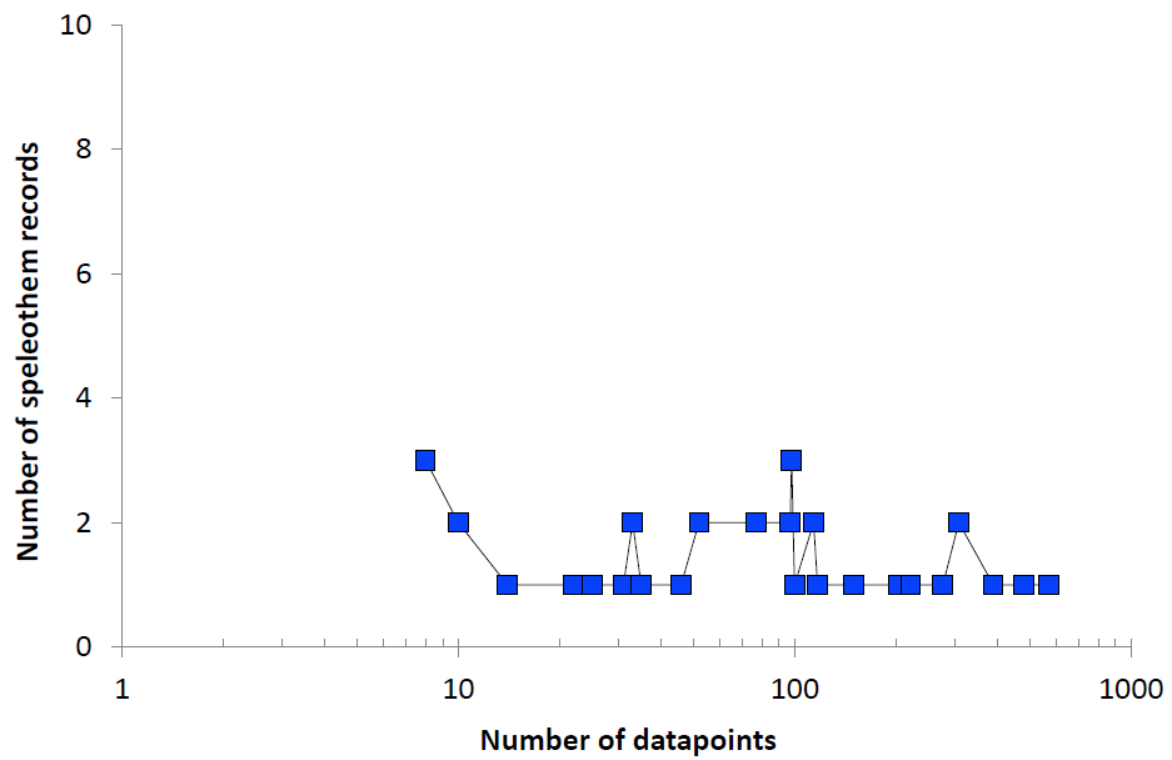


1916 **Figure A4**



1917





1919

1920